Tribofilm Formation of Zinc Dialkyldithiophosphate as Oil Additives Impregnated in Porous Polyimide-Steel Soft Contact

Tribofilm Formation of Zinc Dialkyldithiophosphate as Oil Additives Impregnated in Porous Polyimide-Steel Soft Contact

Zhengrong Xu[1,2], Jinbang Li[1,*], Daniele Botto[2], Kai Li[1], Chenchun Shi[1], Ningning Zhou[3], Tao Qing[3], Yuguo Cui[1]

([1] Ningbo Key Laboratory of Micro-nano Motion and Intelligent Control, Faculty of Mechanical Engineering and Mechanics, Ningbo University, Ningbo 315211, China.

[2] Department of Mechanical and Aerospace Engineering, Politecnico di Torino, Corso Duca degli Abruzzi 24, Torino, 10129, Italy

[3] Beijing Key Laboratory of Long-life Technology of Precise Rotation and Transmission Mechanisms, Beijing Institute of Control Engineering, Beijing 100029, China)

Abstract: As a commonly used lubricant additive, ZDDP can form antiwear tribofilms on metal surfaces, reduce the wear of rolling elements and grooves, and thus holds potential for application in bearing lubrication. However, in the actual operation of bearings using oil-impregnated porous polyimide (iPPI) as the bearing cage, there are both steel-steel contacts and iPPI-steel contacts. The tribofilms formation mechanism of ZDDP under iPPI-steel soft contact remains unclear. Herein, ZDDP was added as a lubricant additive to poly-α-olefin oil (PAO4), and its frictional behavior under soft contact (iPPI-steel) and hard contact (steel-steel) at different temperatures was investigated. Results demonstrated that the rise in temperature leads to an expansion of the area where the ZDDP tribofilms on the worn surface reach their growth limit, and more protective films cover the worn surface, thereby inhibiting the wear of the contact surfaces. FIB-SEM characterization demonstrated that compared with hard contact, the ZDDP tribofilms formed on the steel ball surface under soft contact exhibit stronger continuity and greater thickness, thereby providing more effective protection for the steel ball surface. This study provides necessary insights for the application of ZDDP in bearings with iPPI as the bearing cage.

Key words: porous polyimide; ZDDP; soft contact; bearing cage

*Corresponding author: Jinbang Li. E-mail: lijinbang@nbu.edu.cn;

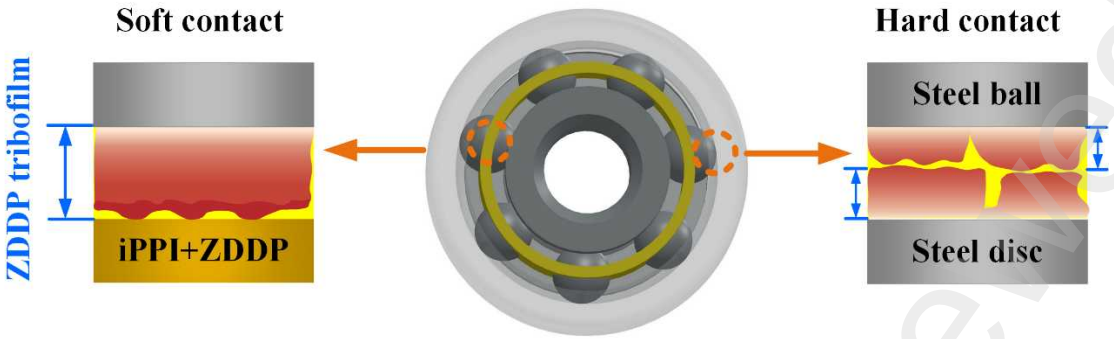

Graphical abstract

1. Introduction

1.1. Background and motivation

Control moment gyroscopes (CMG) are inertial actuators for spacecraft attitude control, and they often operate under conditions of minimum quantity lubrication [1-3]. After prolonged operation, the bearings of the CMG undergo severe wear due to insufficient oil lubrication [4, 5]. Oil-impregnated porous polyimide (iPPI) is an effective approach to providing long-term lubrication [6, 7].

iPPI has a controllable pore size and density, as well as excellent self-lubricating and corrosion -resistance properties. It has also radiation-resistance and shows broad application potential in advanced technologies such as those used in the aerospace industry and micro-oil lubricated rolling bearings [8]. The micropores of iPPI can release stored lubricant under thermal and pressure stimuli and reabsorbs it after stimulus removal, enabling long-term lubrication under conditions of minimum quantity lubrication [9, 10].

However, in practical applications, although iPPI bearing cages can store oil, CMG bearing lubrication still faces the issue of insufficient oil. Effective methods to protect the surfaces of the rolling elements and bearing grooves and reduce their wear, include controlling residual stresses on metal surfaces, modifying contact surfaces and optimizing cage pocket hole shapes.

Studies have found that introducing residual compressive stresses into raceway surfaces via shot peening or ultrasonic surface rolling can delay crack propagation and significantly improve both fatigue resistance and wear resistance of metal surfaces [11, 12]. However, this technology requires

a machining allowance to be retained before the bearing raceways are process to meet the required geometrical tolerances.

Carburizing and nitriding are the two most maturely applied chemical heat treatment technologies [13-15]. Carburizing enhances surface hardness while preserving the impact toughness of the core material. Nitriding improves the wear resistance and corrosion resistance of materials. Ion implantation technology enables functionalities such as friction reduction, anti-wear performance, corrosion resistance, oxidation resistance, and heat resistance without altering dimensional accuracy or surface roughness. In recent years, extensive research has been conducted on ion implantation techniques for bearing steel materials, focusing on ions including Cr, N, C, Ti, and Zr [16-20].

Frequent collisions and wear between the balls and cage pockets during operation make the shape of the cage pockets a significant factor affecting the stability and service life of the bearing. Researchers have found that circular pockets provide the highest stability but result in the largest collision area and wear rate, while rectangular pockets exhibit the lowest wear rate and a high skidding degree [5].

Moreover, using lubricant additives is also a viable approach [21]. Zinc dialkyl dithiophosphate (ZDDP) is a commonly used lubricant additive [22-24]. Under high temperature and metal surface contact, ZDDP decomposes to form a layer of antiwear tribofilms [25-27]. This protective film can cover the metal surface, reduce direct metal-metal contact and thereby reduce the wear of rolling elements and grooves [28-30]. However, in the actual operating of bearings, there are both hard contact (steel-steel) and soft contact (iPPI-steel). The mechanism by which ZDDP forms antiwear tribofilms under soft contact remains unclear. Therefore, it is necessary to study the characteristics of ZDDP film formation under soft contact.

1.2. Objective

The objective of this work is to thoroughly investigate the tribofilm characteristics and formation mechanism of ZDDP under iPPI-steel contact. This study analyzed the differences in morphology of worn surfaces between iPPI-steel and steel-steel contacts, as well as the tribofilm characteristics of ZDDP generated under two contact types. In addition, these analyses can provide necessary reference for the application of ZDDP in bearing lubrication.

This paper is organized as follows. Section 2 provides a detailed description of the materials

used in this study and their material parameters. Friction testing methods and characterization methods are also introduced. Section 3 investigates the tribological characteristics of soft and hard contacts, alongside the characteristics of the ZDDP tribofilm formed under these conditions. It also reveals how the ZDDP tribofilm is formed. Section 4 contains the conclusions and closes the paper.

2. Experiment details

2.1 Materials

Polyimide (thermoplastic polyimide, YS- 20) powders were purchased from Shanghai Synthetic Resin Institute, Shanghai, China. The lubricant, a Synthetic base oil PAO4, was purchased from INEOS Group Holdings Ltd., London, UK, with a kinematic viscosity of 17.4 mm^2/s at 40 °C and a density of 0.82 g/cm^3. The additive ZDDP (T203) was purchased from Bett Chemical Co., Ltd, Jinzhou, China.

The material characteristic and geometry of the steel ball, the steel disc and the porous polyimide (PPI) disc are shown in Table 1. Both the disc and the balls are made GCr15 (AISI 52100) steel. The PPI discs were prepared by cold-pressing and hot-sintering methods. The PPI discs were immersed in PAO4 oil with a ZDDP concentration of 2 wt% in a vacuum oven under the pressure of 20 Pa and temperature of 80 ℃ for 20 h to obtain iPPI. The oil content was around 11 wt%.

Table 1. Material characteristic and geometry

Contact Materials	Diameter/Thickness (mm)	Density (g/cm^3)	Poisson's ratio	Hardness	Elastic Modulus (GPa)	Surface Roughness, Ra
Steel ball	Φ6	7.3	0.3	63 HRC	208	10 nm
Steel disc	Φ10 / 3	7.3	0.3	200 HV30	208	20 nm
PPI disc	Φ10 / 3	1.1	0.37	78-84 Shore D	1.14	0.35 μm

2.2 Tests and Characterizations

The friction tests were carried out on a high frequency reciprocating friction tester (CMS-01,

Beijing Chaoyang high tech Applied Technology Research Institute Co., Ltd, China), with the reciprocating frequency set at 50 Hz, a load of 2 N, and a stroke of 1 mm. The physical diagram, schematic diagram of the testing machine, and material contact schematic diagram are shown in Fig. 1. Four different temperatures were applied: 40 ℃, 80 ℃, 120 ℃, and 160 ℃, respectively. Each friction test lasted for three hours, involved 540,000 cycles and was repeated three times under the same conditions. A previous study found that adding 2 wt% ZDDP to pure PAO4 effectively reduced the wear in steel-steel contacts [31]. Therefore, in this study we used PAO4 with a ZDDP concentration of 2 wt%. It is worth noting that the discs were completely submerged in lubricating oil throughout the entire experiment. In addition, in order to investigate the ZDDP tribofilm characteristics under soft contact, the characteristics of ZDDP tribofilm under hard contact were also studied and compared.

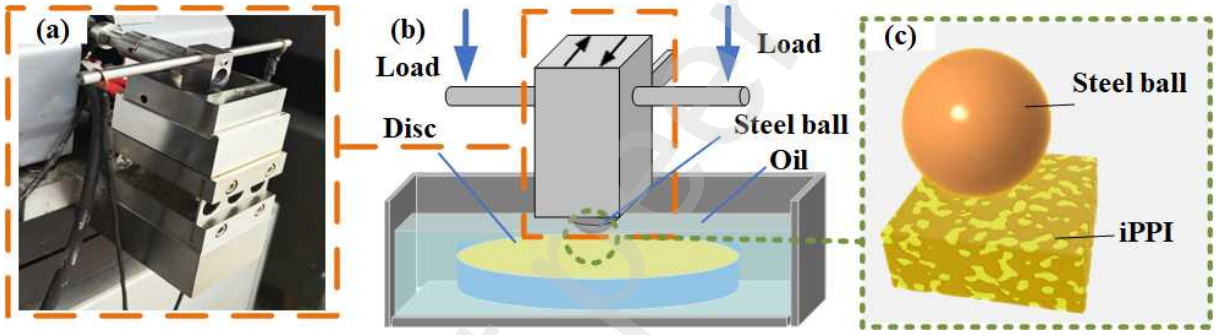

Fig. 1 High frequency reciprocating friction tester: (a) Test physical diagram, (b) Test schematic diagram, (c) Material contact schematic diagram.

The morphology of the worn surfaces was observed by an optical microscope (KH-8700, HIROX) and a laser confocal microscope (LSM900, Zeiss, Germany). Scanning electron microscopy (SEM SU5000, Hitachi, Japan) was employed to detect the surfaces and EDS (Ultim MAX, 100 mm^2) was used to analyze the elemental content and distribution of the worn surfaces. The worn surfaces were also characterized by Raman spectroscopy (Alpha 300 RA, WITec, Germany) to analyze the chemical composition. The continuity and thickness of the ZDDP tribofilms formed on the surface of steel balls were analyzed by a focused ion beam-scanning electron microscope (FIB-SEM).

3. Results and Discussion

3.1 Tribological characteristics of soft contact

The friction and wear characteristics under soft contact at different temperatures are shown in

Fig. 2. The average friction coefficients under soft contact are shown in Fig. 2 (a). As the temperature increases, the average friction coefficient under both conditions initially increases and then stabilizes, reaching their peak value at 120 °C. This result is consistent with the conclusions drawn in Ref. [32]. The average friction coefficient under lubrication with PAO4 containing 2 wt% ZDDP was consistently lower than that under pure PAO4 lubrication below 120 °C.

An optical microscope was used to measure the size of the surface worn area of steel balls at different temperatures, and the measurement results are shown in Fig. 2 (b). As the temperature increases, the size of the worn area on the surface of the steel ball under soft contact gradually increases under both lubrication conditions.

Due to the discontinuity of the ZDDP tribofilms, its coverage area is considered to be smaller than the size of the worn area of the steel ball under lubrication with PAO4 containing 2 wt% ZDDP. The change in the coverage area of the ZDDP tribofilms on the surface of the steel ball also show a similar trend. For soft contact, the elastic modulus of the PPI disc (approximately 2 GPa) is much lower than that of ZDDP tribofilms (higher than 15 GPa), and its hardness (approximately 78 Shore D) is also significantly lower than that of ZDDP tribofilms (higher than 1.5 GPa) [30, 33, 34]. Furthermore, molecular dynamics simulations reveal that the interfacial diffusion between the tribofilms and oxide layer leads to increased hardness of the friction film, thereby enhancing its resistance to shear forces [27, 35, 36]. Consequently, under soft contact, the ZDDP tribofilms covering the steel ball surface become difficult to remove, the coverage area of ZDDP tribofilms on the steel ball surface increases progressively.

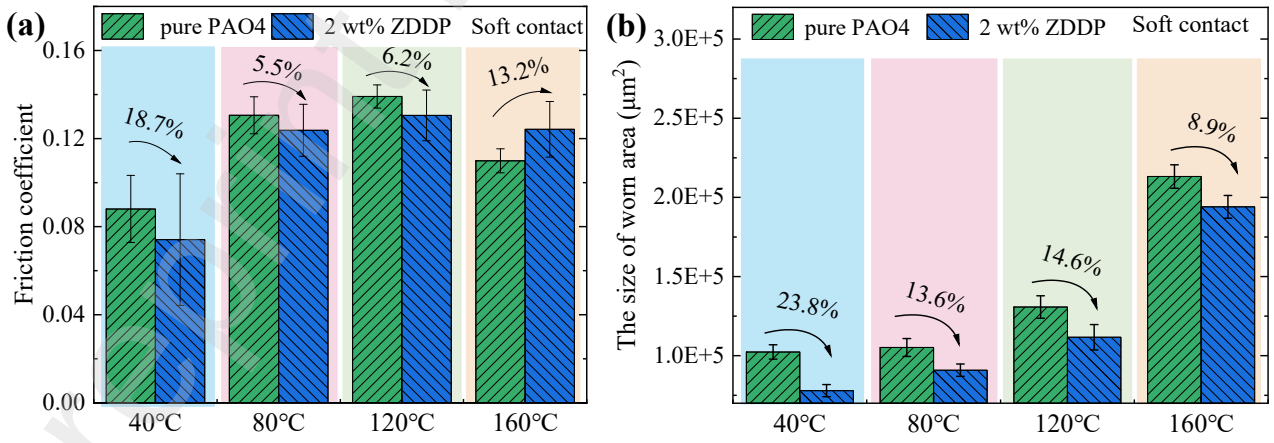

Fig. 2 Friction and wear characteristics under soft contacts: (a) the average friction coefficients at different temperatures under soft contact, (b) the size of worn area of steel balls at different temperatures under soft contact.

The worn surfaces of the steel balls under soft contact were observed using optical microscopy, and are shown in Fig. 3 (a1-d1). Enlarged detail of the worn area of the steel ball are shown in Fig. 3 (a2-d2). Under pure PAO4 lubrication, it can be found that as the temperature increases, the size of the worn area on the surface of the steel ball gradually increases, and there are also wear marks in the worn area on the surface of the steel ball. Figure 3 (a3-d3) shows the worn surfaces of steel balls under soft contact (2 wt% ZDDP). The details of the worn area on the surface of the steel ball are shown in Fig.3 (a4-d4). As the temperature increases, the areas in which ZDDP tribofilms form on the surface of the steel ball gradually increase. This growth can be divided into two stages. The coverage of ZDDP tribofilms gradually increases from 40 °C to 80 °C but the tribofilms primarily consists of discontinuous, pad-like structures, as shown in Fig.3 (a4-d4). At higher temperatures (between 120 °C to 160 °C), ZDDP tribofilms cover a greater area of wear, with both pad-like and continuous tribofilms increasing progressively.

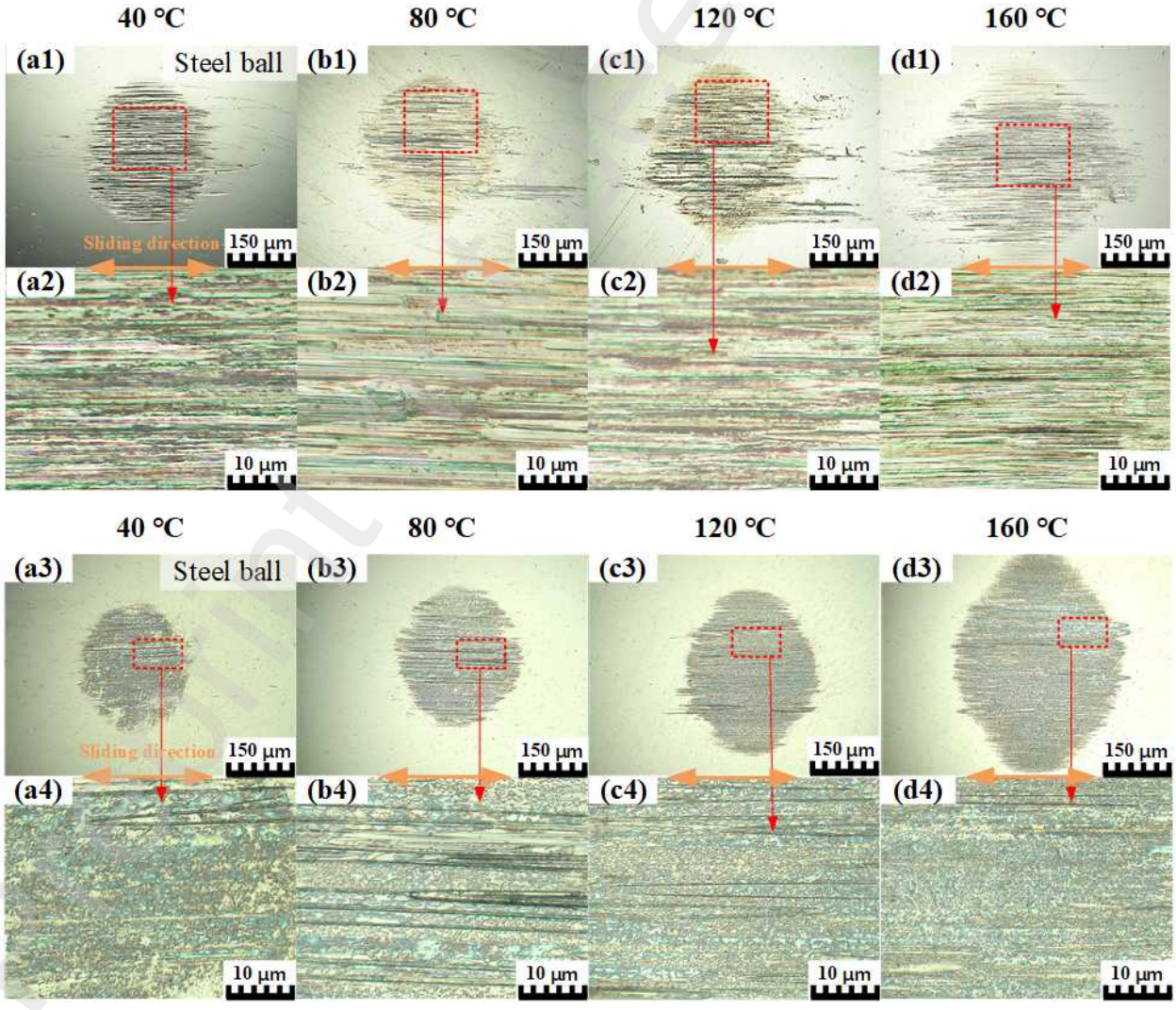

Fig. 3 The worn surfaces of steel balls under soft contact: (a1-d1) the worn surfaces of steel balls at different temperatures (pure PAO4), (a2-d2) enlarged detail of the worn area of the steel balls at different temperatures (pure PAO4), (a3-d3) the worn surfaces of steel balls at different temperatures (2 wt% ZDDP), (a4-d4) enlarged detail of the worn area of the steel balls at different temperatures (2 wt% ZDDP).

The laser confocal microscope was used to characterize the profiles of the worn surfaces of steel balls under soft contact, and the results are shown in Fig. 4 (a) and 4 (b), respectively. Under pure PAO4 lubrication, the circular arc profile curves of the steel ball surfaces have obvious fluctuations, and the circular arc shape is not complete. This indicates that wear has modified the geometry of the surface of the steel ball. Under the condition of adding 2 wt% ZDDP as a lubricant in PAO4, as the temperature increases, the length of the rough section on the surface of the steel ball profiles curves gradually increases, but the roughness is similar (see Table 2). At 160 ℃, the length of the rough segment is the longest and the roughness is also the highest.

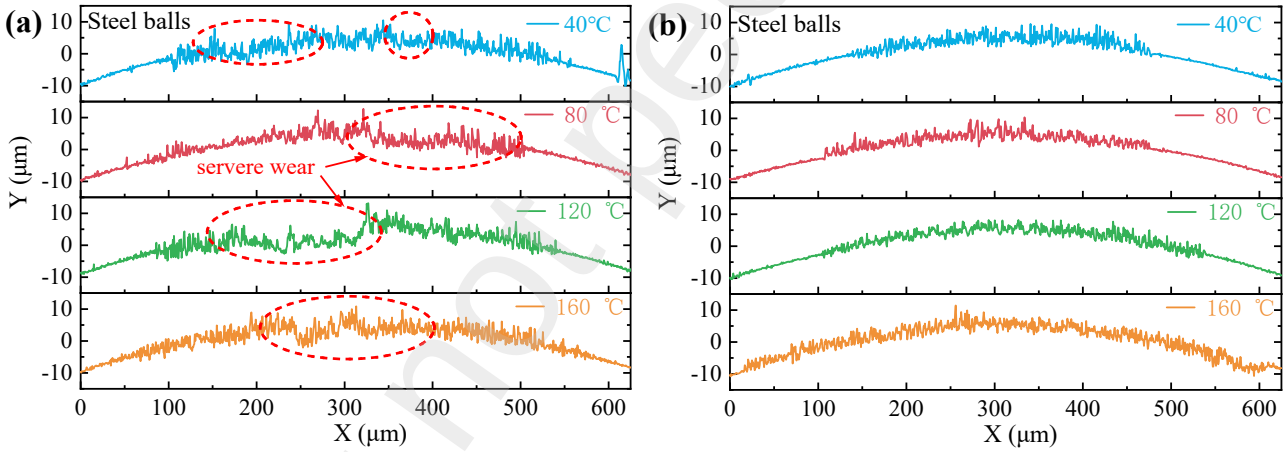

Fig. 4 The profiles of worn surfaces of steel balls under soft contact: (a) the profiles curves of steel balls at different temperatures (pure PAO4), (b) the profiles curves of steel balls at different temperatures (2 wt% ZDDP).

The worn surfaces of PPI discs under soft contact are shown in Fig. 5. Figure 5 (a1-d1) shows the worn surfaces of PPI discs under soft contact (pure PAO4). Enlarged detail of the worn area of the PPI discs are shown in Fig. 5 (a2-d2). As the temperature rises, the width of the wear scar on the PPI disc gradually increases. Meanwhile, the blackening wear on the worn surface of PPI is becoming increasingly severe. This is attributed to the iron oxides generated on the worn surface of the steel ball, which cause blackening of the worn surface.[6]

Fig. 5 (a3-d3) shows the worn surfaces of PPI discs under soft contact (2 wt% ZDDP). Enlarged detail of the worn area of the PPI discs are shown in Fig. 5 (a4-d4). As the temperature rises, the area where ZDDP tribofilms on the surface of the steel ball reaches its growth limit gradually increases, leading to an increase in the width of the wear scar of PPI. The growth limit is the maximum size of the coverage area. Interestingly, blackening wear can still be observed on the worn surface of PPI, which may be caused by PPI collecting excess debris formed by ZDDP tribofilms.

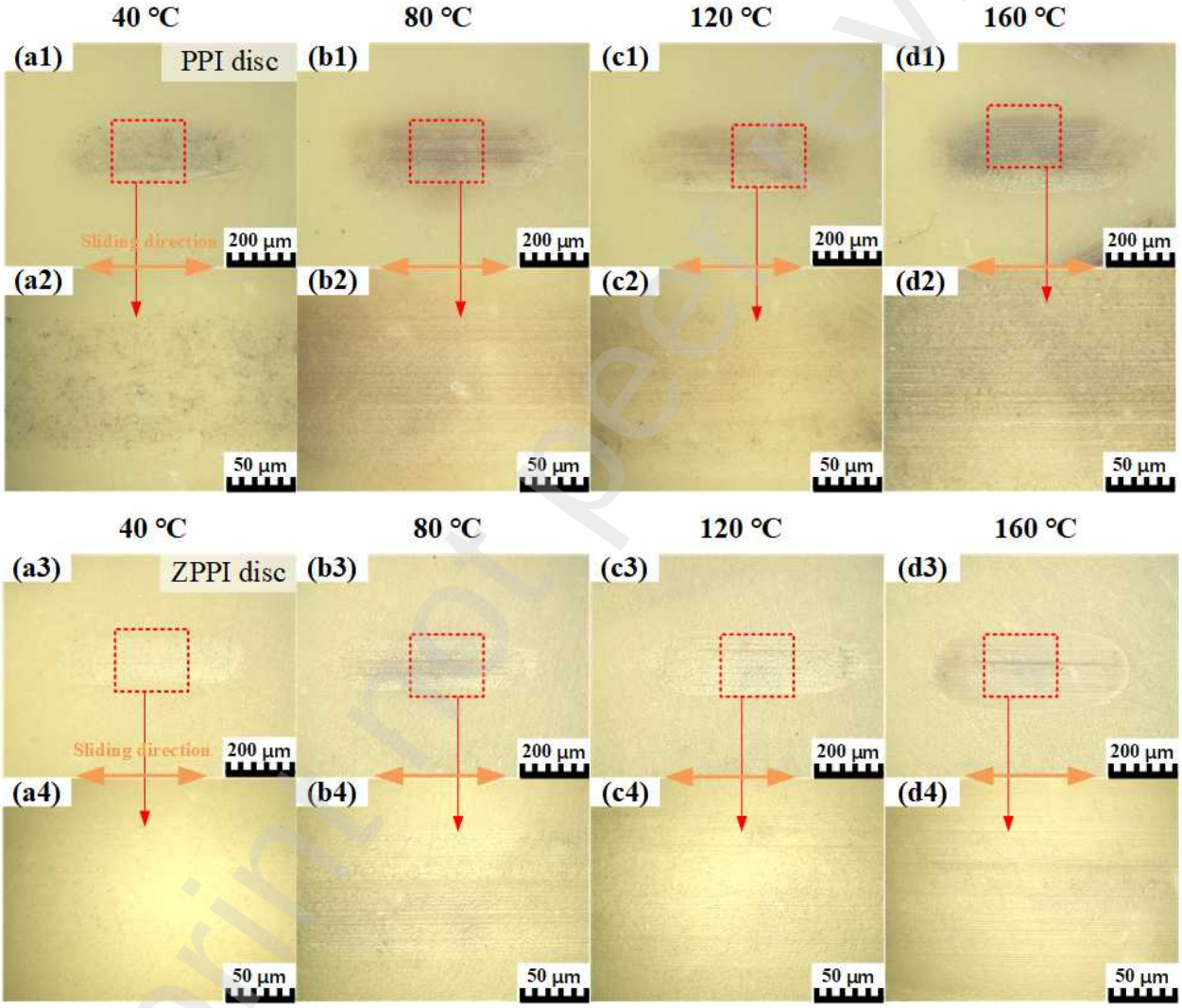

Fig. 5 The worn surfaces of PPI discs under soft contact: (a1-d1) the worn surfaces of PPI discs at different temperatures (pure PAO4), (a2-d2) enlarged detail of the worn area of the PPI discs at different temperatures (pure PAO4), (a3-d3) the worn surfaces of PPI discs at different temperatures (2 wt% ZDDP), (a4-d4) enlarged detail of the worn area of the PPI discs at different temperatures (2 wt% ZDDP).

The profiles of the worn surfaces of PPI discs under soft contact are shown in Fig. 6 (a) and 6 (b), respectively. Under pure PAO4 lubrication, as the temperature rises, the wear depth on the surface of the PPI discs gradually increases, reaching a maximum of 9 μm. Under the condition of adding 2 wt% ZDDP as a lubricant in PAO4, the wear of PPI is negligible at 40 °C. From 80 °C to 160 °C, the wear of the PPI disc becomes increasingly severe, with the maximum wear depth reaching 10 μm. On one hand, the increase in temperature reduces the viscosity of the lubricating oil. On the other hand, the rise in temperature may cause the PPI surface to soften, thereby increasing wear.

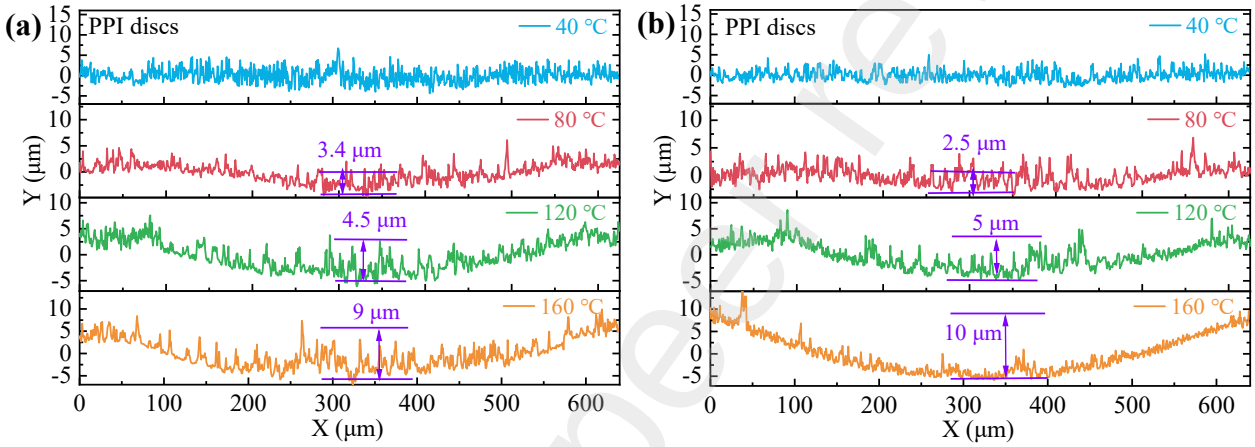

Fig. 6 The profiles of worn surfaces of PPI discs under soft contact: (a) the profiles curves of PPI discs at different temperatures (pure PAO4), (b) the profiles curves of PPI discs at different temperatures (2 wt% ZDDP).

3.2 Tribological characteristics of hard contacts for comparison

The friction and wear characteristics under hard contact at different temperatures are shown in Fig. 7. The average friction coefficients under hard contact are shown in Fig. 7 (a). As the temperature rises, both the average friction coefficient under pure PAO4 lubrication conditions and that with 2 wt% ZDDP added to PAO4 initially increase and then tend to stabilize. It is worth noting that across all four test temperatures, the ZDDP-modified PAO4 maintains a significantly lower COF than pure PAO4. The maximum reduction reached 28.4 wt% at 120 °C.

The size of the surface worn area of steel balls at different temperatures under hard contact are shown in Fig. 7 (b). It can be found that at any temperature, the size of the worn area of steel balls with 2 wt% ZDDP added as lubricant in PAO4 is always lower than that with pure PAO4 as lubricant. As the temperature rises, the size of the worn area on the surface of the steel ball shows different

variation patterns under two different lubrication conditions. Under pure PAO4 lubrication, the size of the worn area on steel balls gradually increased with rising temperature. Conversely, under the condition of adding 2 wt% ZDDP as a lubricant in PAO4, as the temperature increases, the size of the worn area on the surface of the steel ball initially decreases and then increases. This behaviour is the result of an increased formation of ZDDP tribofilms at higher temperatures. These tribofilms effectively protected the steel surfaces and reduced wear.

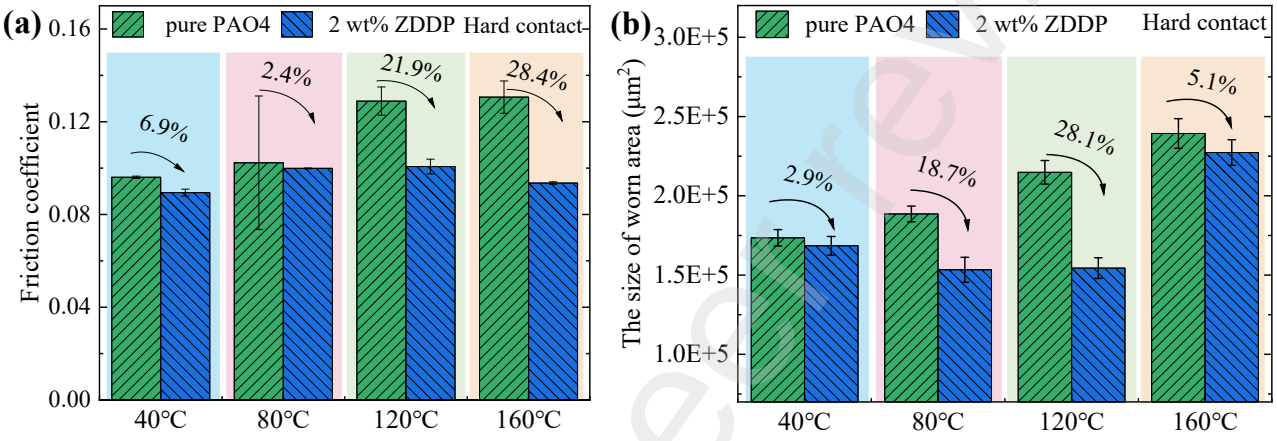

Fig. 7 Friction and wear characteristics under hard contacts: (a) the average friction coefficients at different temperatures under hard contact, (b) the size of worn area of steel balls at different temperatures under hard contact.

It is worth noting that at the same temperature, the size of coverage area of ZDDP tribofilms on the surface of steel balls under hard contact is always bigger than that under soft contact (Fig. 2 (b)). This is because metal surfaces have high activity, while polymer surfaces are usually relatively inert, with low chemical activity and weak reactivity with ZDDP decomposition products, which is not conducive to the rapid formation of ZDDP tribofilms.

Figure 8 shows the worn surfaces of steel balls under hard contact. Figure 8 (a1-d1) shows the worn surfaces of steel balls under hard contact (pure PAO4). Enlarged detail of the worn area of the steel balls are shown in Fig. 8 (a2-d2). As the temperature increases, the size of the worn area on the surface of the steel ball gradually increases, and there is material peeling in the worn area on the surface of the steel ball. Figure 8 (a3-d3) shows the worn surfaces of steel balls under hard contact (2 wt% ZDDP). The details of the worn area on the surface of the steel ball are shown in Figure 8 (a4-

d4). It is evident that the area where the ZDDP tribofilms reach their growth limit changes with rising temperature. This area initially shrinks and then expands, a process that can be broadly divided into two distinct phases. There is a slight decrease in the area where the ZDDP tribofilm on the worn surface of the steel ball reaches its growth limit when the temperature ranges from 40 ℃ to 120 ℃.

As the temperature rises to 160 ℃, the coverage area of ZDDP tribofilms on the worn surface of the steel ball increases significantly. At the same time, the steel ball experiences significantly increased wear. Compared to the worn surface at 120 ℃, the removal rate of the pad-like film within the worn area increased, even though the coverage area of ZDDP tribofilms on the steel ball surface also increased at 160 ℃.

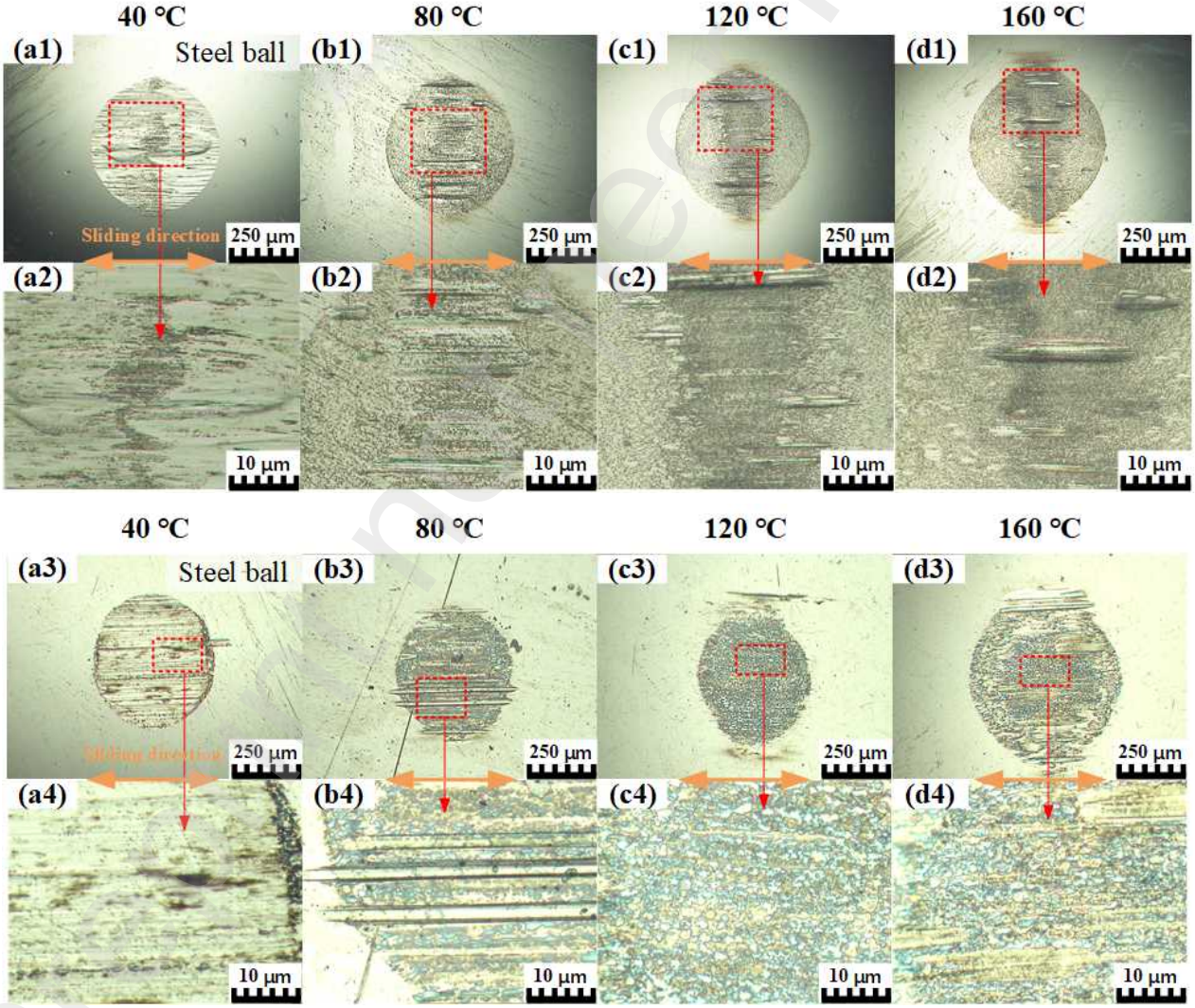

Fig. 8 The worn surfaces of steel balls under hard contact: (a1-d1) the worn surfaces of steel balls at different temperatures (pure PAO4), (a2-d2) enlarged detail of the worn area of the steel balls at different temperatures

(pure PAO4), (a3-d3) the worn surfaces of steel balls at different temperatures (2 wt% ZDDP), (a4-d4) enlarged detail of the worn area of the steel balls at different temperatures (2 wt% ZDDP).

The profiles of the worn surfaces of steel balls under hard contact are shown in Fig. 9 (a) and 9 (b), respectively. When 2 wt% ZDDP is added as a lubricant to PAO4, the worn surfaces of the steel balls become very rough due to the formation of ZDDP tribofilms. However, the diameter of the wear scar on the steel ball does not increase as the viscosity of the lubricating oil decreases due to an increase in temperature. The wear scar diameter of the steel ball can be calculated from the profile curve (1024 data points in total). The diameter of the wear scar on the steel ball surface first decreases and then increases. This indicates that the formed ZDDP tribofilm can protect the steel balls surface and reduce wear.

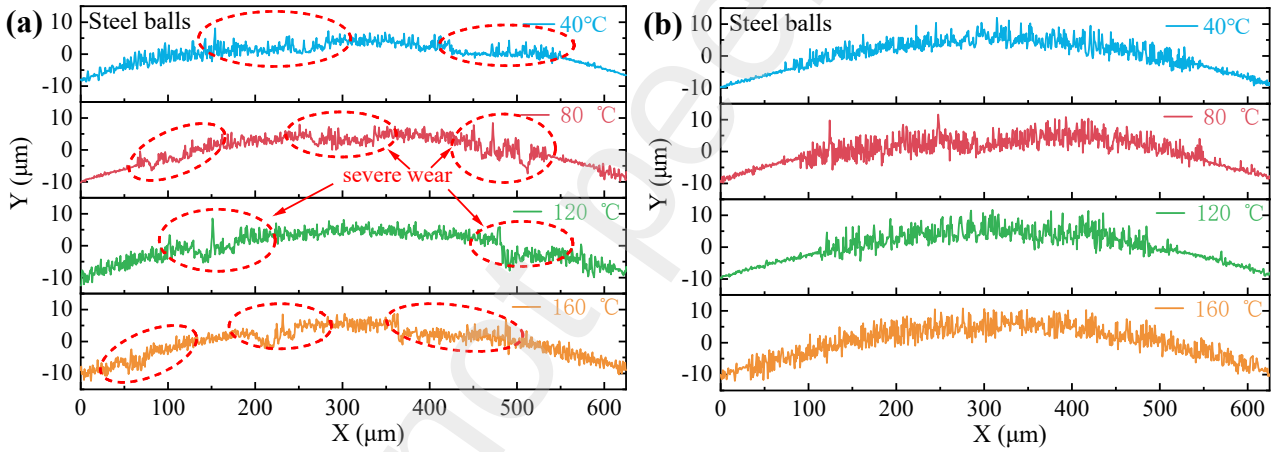

Fig. 9 The profiles of worn surfaces of steel balls under hard contact: (a) the profiles curves of steel balls at different temperatures (pure PAO4), (b) the profiles curves of steel balls at different temperatures (2 wt% ZDDP).

Figure 10 (a1-d1) shows the worn surfaces of steel discs under hard contact (pure PAO4), while Figure 10 (a2-d2) shows the worn profiles. As the temperature rises, the width of the wear scar on the steel disc gradually increases. An increase in temperature leads to a decrease in the viscosity of the lubricant, which reduces the load-bearing capacity of the oil film. This results in the wear scar width on the steel disc gradually widening.

Figure 10 (a3-d3) illustrates the wear patterns on the surfaces of the steel discs when subjected to hard contact with 2 wt% ZDDP. Enlarged detail of the worn area of the steel discs are shown in

Fig. 10 (a4-d4). As the temperature rises, the width of the wear scar on the steel disc also gradually increases. On the one hand, an increase in temperature makes the lubricant more fluid, which allows the ZDDP molecules to disperse more easily into the contact area. On the other hand, it also promotes the spreading and film formation of reaction products on the steel ball surface, making the ZDDP tribofilms easier to form and grow.

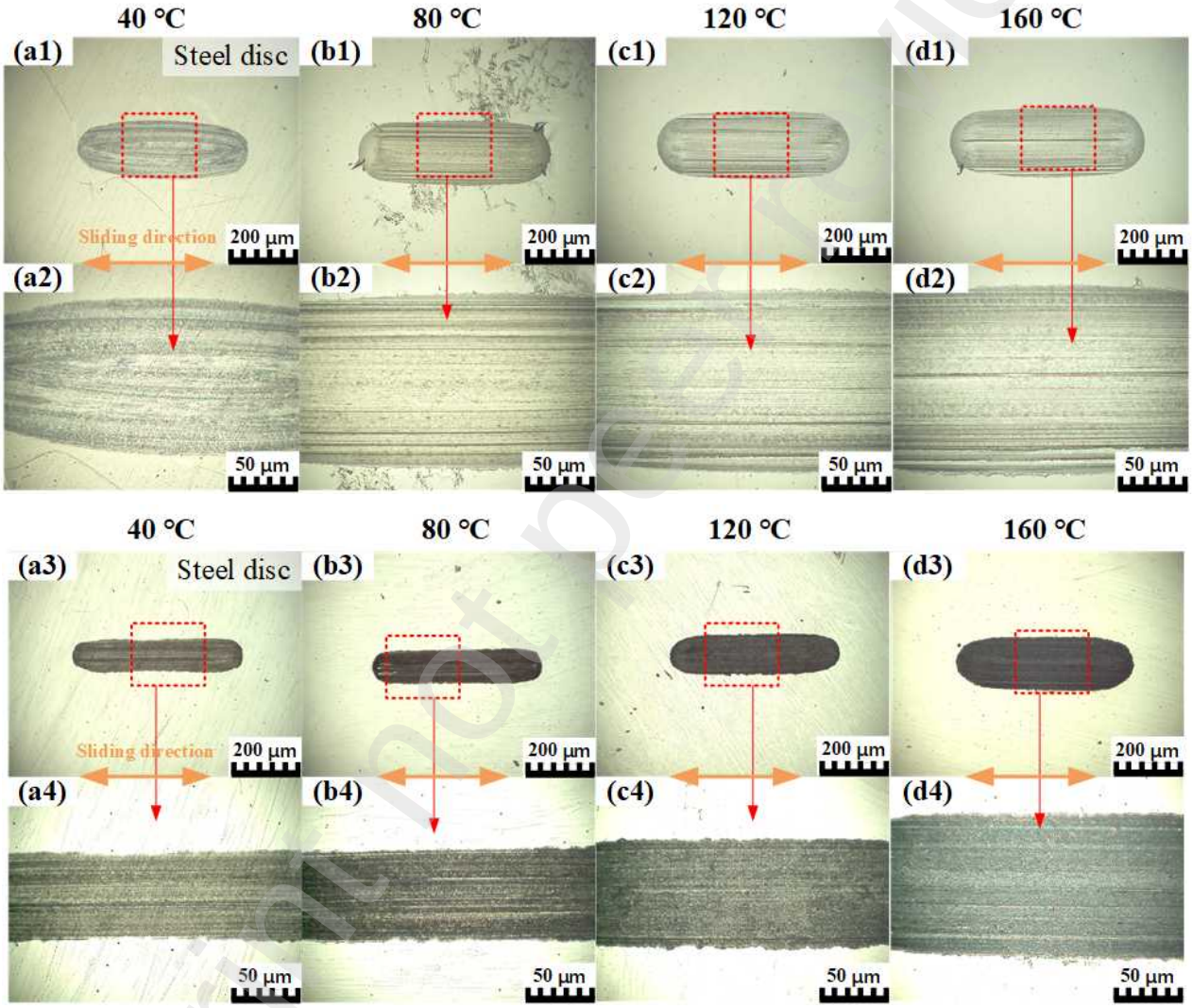

Fig. 10 The worn surfaces of steel discs under hard contact: (a1-d1) the worn surfaces of steel discs at different temperatures (pure PAO4), (a2-d2) enlarged detail of the worn area of the steel discs at different temperatures (pure PAO4), (a3-d3) the worn surfaces of steel discs at different temperatures (2 wt% ZDDP), (a4-d4) enlarged detail of the worn area of the steel discs at different temperatures (2 wt% ZDDP).

The profiles of the worn surfaces of steel discs under hard contact are shown in Fig. 11 (a) and

11 (b), respectively. Under pure PAO4 lubrication, the wear depth on the surface of the steel discs gradually increases, reaching a maximum of 7.2 μm at 160 °C. Under the condition of adding 2 wt% ZDDP as a lubricant in PAO4, the generated ZDDP tribofilms reduced the wear on the surface of the steel discs. The smooth segments on both sides of the profile curve represent the unworn regions of the steel disc, while the rough segments correspond to the worn regions (Fig. 11 (b)). From 40 °C to 120 °C, although the worn area on the surface of the steel disc increased, the depth of the wear scars did not increase. Additionally, the profiles curves of the worn area were higher than that of the original surface. This indicates that the protective film covers the surfaces of the steel ball and steel disc, avoiding direct contact between them. At 160 °C, the depth and width of the wear scar on the steel disc significantly increase, with the deepest point reaching 4 μm.

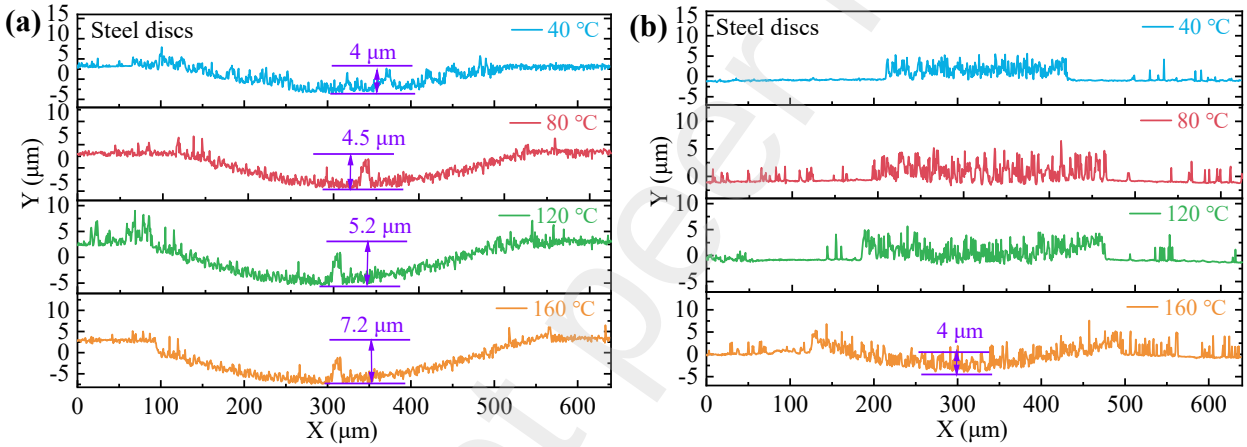

Fig. 11 The profiles of worn surfaces of steel discs under hard contact: (a) the profiles curves of steel discs at different temperatures (pure PAO4), (b) the profiles curves of steel discs at different temperatures (2 wt% ZDDP).

Table 2 Roughness (Ra) of the worn surfaces of balls and discs under soft and hard contact at different temperatures (2 wt% ZDDP)

Worn area	40 °C (μm)	80 °C (μm)	120 °C (μm)	160 °C (μm)
Steel ball (soft contact)	0.7496	0.7226	0.7328	0.8314
PPI disc	0.8202	0.8862	0.9842	1.6225
Steel ball (hard contact)	0.7993	0.8538	0.8015	0.8941
Steel disc	0.7823	0.8401	0.8985	0.9648

Although an oil film can form on the contact surface between the PPI disc and the steel ball under rich oil lubrication conditions, the contact remains in a boundary lubrication state due to the high roughness of the contact surfaces. This can be calculated through the film thickness ratio (λ). Based on the Dowson and Hamrock film thickness equations [37], the thickness of the oil film (h_{min}) can also be calculated. The formulas for λ and the thickness of the oil film are as follows:

$$\lambda = \frac{h_{\min}}{\sqrt{R_{q1}^2 + R_{q2}^2}} \tag{1}$$

$$h_{min} = 3.63 \frac{G^{*0.49} U^{*0.68}}{W^{*0.073}} \left(1 - e^{-0.68k}\right) \tag{2}$$

where h_{min} is the minimum oil film thickness, G^* is the material parameter, U^* is the velocity parameter, and W^* is the load parameter, R_{q1} is the RMS surface roughness of the PPI disc (for the soft contact) or the steel disc (for the hard contact), and R_{q2} is the RMS surface roughness of the steel ball.

The minimum oil film thickness under soft contact (2 wt% ZDDP) and hard contact (2 wt% ZDDP) is 6.63 nm and 6.39 nm, respectively. As the temperature increases, the viscosity of the lubricating oil gradually decreases, and the thickness of ZDDP tribofilms will gradually decrease. Therefore, the oil film thickness is the highest at 40 ℃. The λ values of soft contact (2 wt% ZDDP) and hard contact (2 wt% ZDDP) are 0.0059, and 0.0057 (40 ℃), indicating that the contacts are essentially in a boundary lubrication state.

3.3 Characteristics of ZDDP tribofilms under soft contact

The worn surfaces of steel balls under soft contact (2 wt% ZDDP) were observed by SEM to further analyze the effect of temperature on generating of ZDDP tribofilms are shown in Fig. 12. As the temperature increases, the pad-like ZDDP tribofilms in the worn area on the steel ball surface becomes increasingly dense. Meanwhile, its continuity is also enhanced. The distribution and content of the elements on the worn surfaces under soft contact were examined by EDS are shown in Fig. 12. The contents of typical elements are shown in Table 3. As the temperature increases, the content of typical elements in the ZDDP tribofilms, such as sulfur (S), zinc (Zn), and phosphorus (P), gradually increases. This indicates that temperature promotes the formation of the ZDDP tribofilms. The increase in Zn content was the most significant, increasing by 10.17 wt% from 40 ℃ to 120 ℃, while

the increase in S content was the weakest, only increasing by 0.5 wt%.

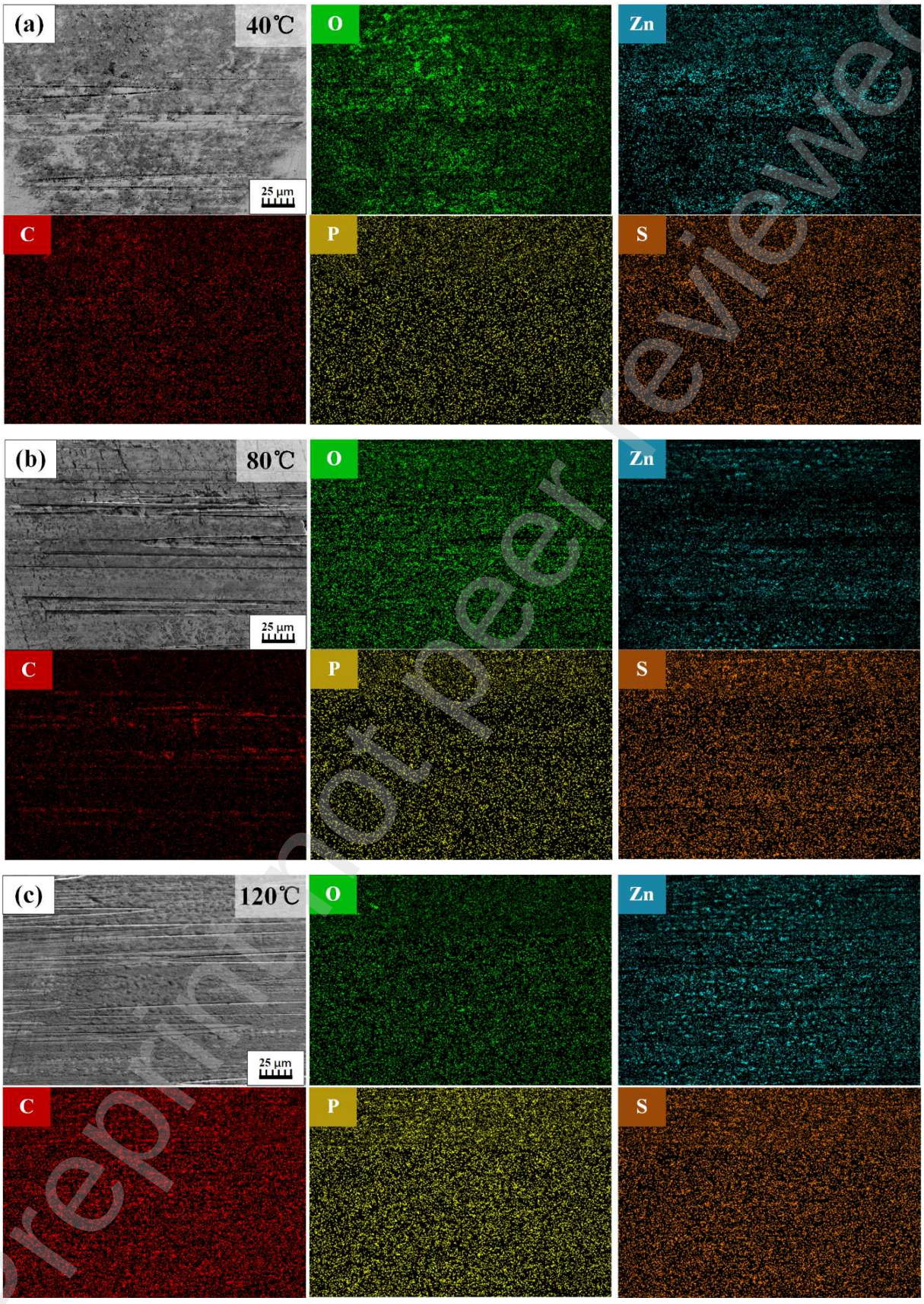

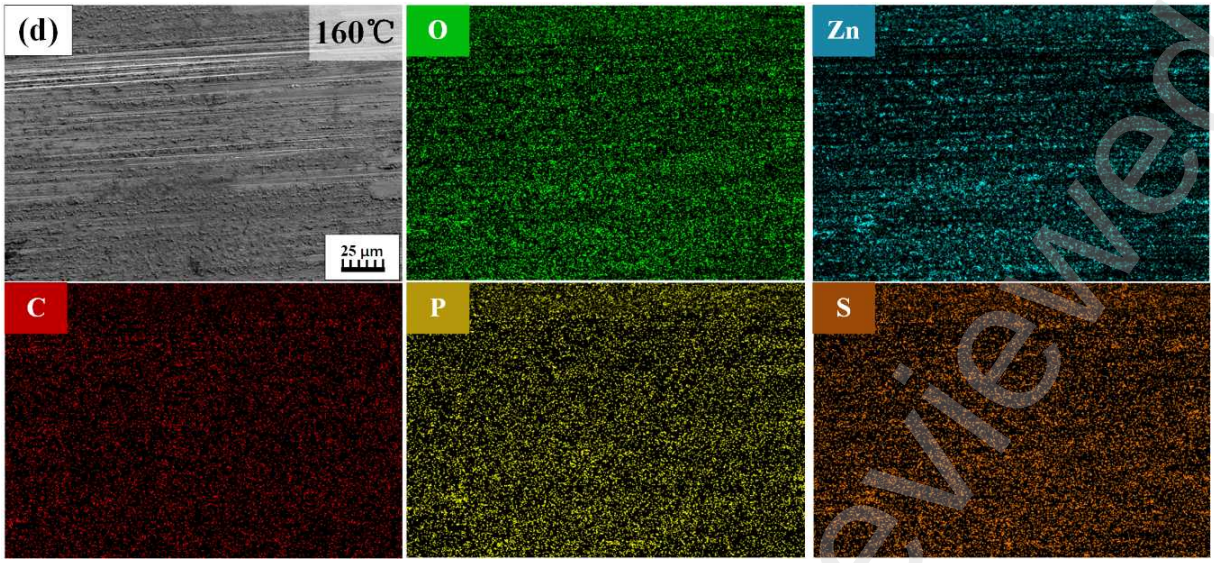

Fig.12 Microstructure and elemental maps of worn surfaces on steel ball under soft contact at different temperatures: (a) 40 ℃, (b) 80 ℃, (c) 120 ℃, (d) 160 ℃

Table. 3 Content of characteristic elements on the worn surface of soft contact

Temperature (℃)	Fe (%)	C (%)	O %)	Zn (%)	P (%)	S (%)
40	86.44	6.39	3.02	3.81	0.04	0.30
80	85.46	6.49	1.68	5.71	0.16	0.50
120	82.10	6.16	2.63	7.75	0.67	0.69
160	75.83	5.08	3.22	13.98	1.09	0.80

Fig. 13 compares the morphology of ZDDP tribofilms formed on the worn surfaces of steel balls under soft and hard contacts at the same temperature (160 ℃). It can be observed that under soft contact, the pad-like ZDDP tribofilms on the steel ball surface is mostly composed of continuous dots, with each individual film having a relatively small area but appearing to be thicker. In contrast, under hard contact, the area of each pad-like ZDDP tribofilms on the steel ball surface is significantly larger, but the film thickness is lower. The content of characteristic elements on the worn surface of soft and hard contact is shown in Table 4. At the same temperature and pressure, the characteristic element content of ZDDP tribofilms on the worn surface of steel balls under soft contact is higher. This indicates that steel balls are better protected under soft contact, resulting in lower wear.

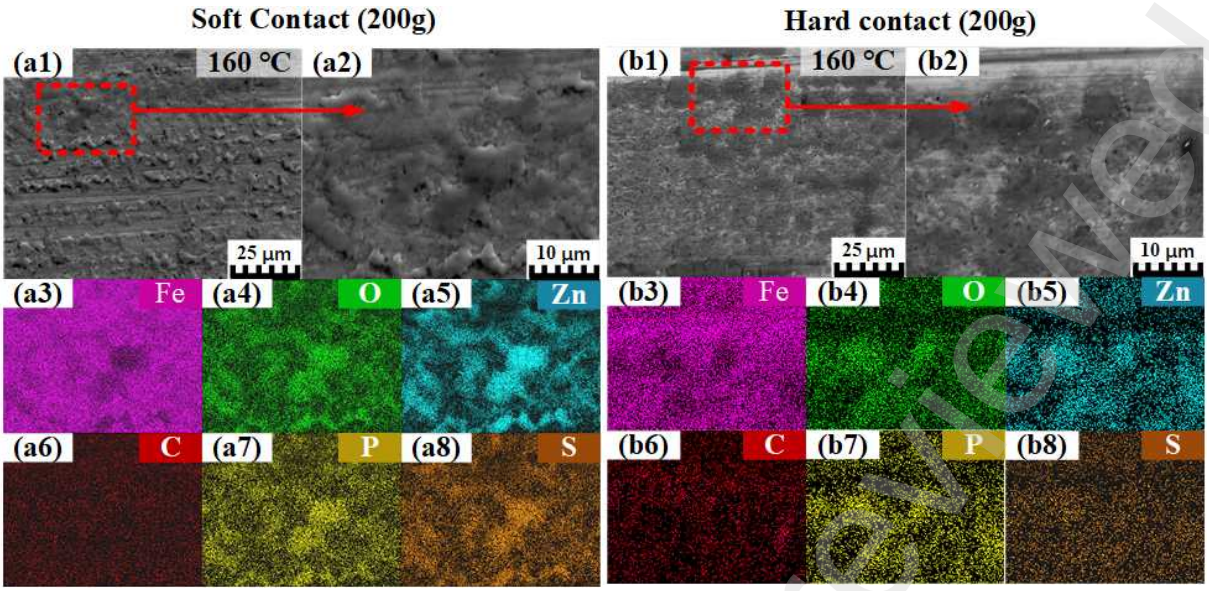

Fig.13 Microstructure and elemental maps of worn surfaces on steel ball under soft contact at same temperature: (a1-a8) soft contact, (b1-b8) hard contact

Tab. 4 The content of characteristic elements on the worn surface of soft and hard contact (2 wt% ZDDP)

Contact type	Fe (%)	C (%)	O (%)	Zn (%)	P (%)	S (%)
Soft contact	70.35	4.85	4.05	18.15	1.16	1.44
Hard contact	82.43	4.21	4.31	6.64	1.05	1.36

The worn area on the surfaces of the steel balls under soft contact were examined by a Raman spectroscopy. The results are shown in Fig. 14. Compared with the worn steel ball surface under pure PAO4 conditions, it is difficult to find characteristic peaks of iron oxides on the surface of steel balls, such as Fe_2O_3 (223 cm^{-1},292 cm^{-1},409 cm^{-1},1317 cm^{-1}), except for the weak peak of Fe_3O_4 (650 cm^{-1}) [38, 39]. This indicates that ZDDP inhibits the formation of iron oxides. The characteristic peak of sulphide (337 cm^{-1}, 367 cm^{-1}) and phosphate (close to 1033 cm^{-1}) can be detected on the worn surface of steel balls at all four temperatures [40,41]. It is worth noting that the peak of sulphide is significantly higher than that of phosphate, which is contrary to the EDS results. This may be due to the weaker sensitivity of Raman spectroscopy to phosphates. In addition, the intensity of the D and G peaks in the spectrum is very high [42]. Furthermore, under high-temperature conditions (above 80 °C), the intensities of the D and G in the spectra are extremely high. Based on the wear morphology of the PPI surface, it can be inferred that, on one hand, the D and G may originate from the debris of

PPI. On the other hand, Fe_3O_4 catalyzes the decomposition of PAO4 [43].

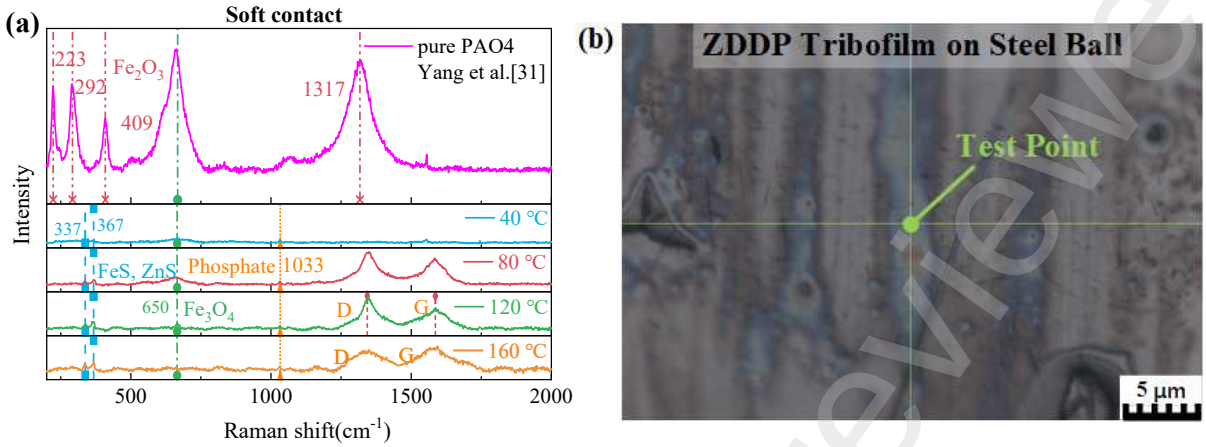

Fig.14 Raman examination results of steel balls worn surfaces at different temperatures: (a) Raman spectra on the worn surface of steel balls at different temperatures, from top to bottom, the temperatures are 40 ℃, 80 ℃, 120 ℃ and 160 ℃, respectively, (b) detection areas on the worn surfaces of the steel balls.

In order to further study the characteristics of ZDDP tribofilms generated on the worn surface of steel balls under soft and hard contact, FIB-SEM was used to detect the thickness of the film are shown in Fig. 15. The black base at the bottom of the image is the steel ball, the white area at the top is the protective tungsten coating, and the region outlined by the orange dashed line in the middle is the ZDDP tribofilms (see Fig. 15(a)). Three areas within the ZDDP tribofilms region were selected to calculate the average film thickness. The results indicate that under soft contact, the average thickness of the ZDDP tribofilms is 216.8 nm, while under hard contact, the average thickness of the ZDDP tribofilms is 145.54 nm, which is lower than that under soft contact (see Fig. 15(b)). It is worth noting that under soft contact, the ZDDP tribofilm exhibits stronger continuity. This may be due to the lower hardness of the PPI disc compared to the steel disc under soft contact, making the ZDDP tribofilm less prone to wear.

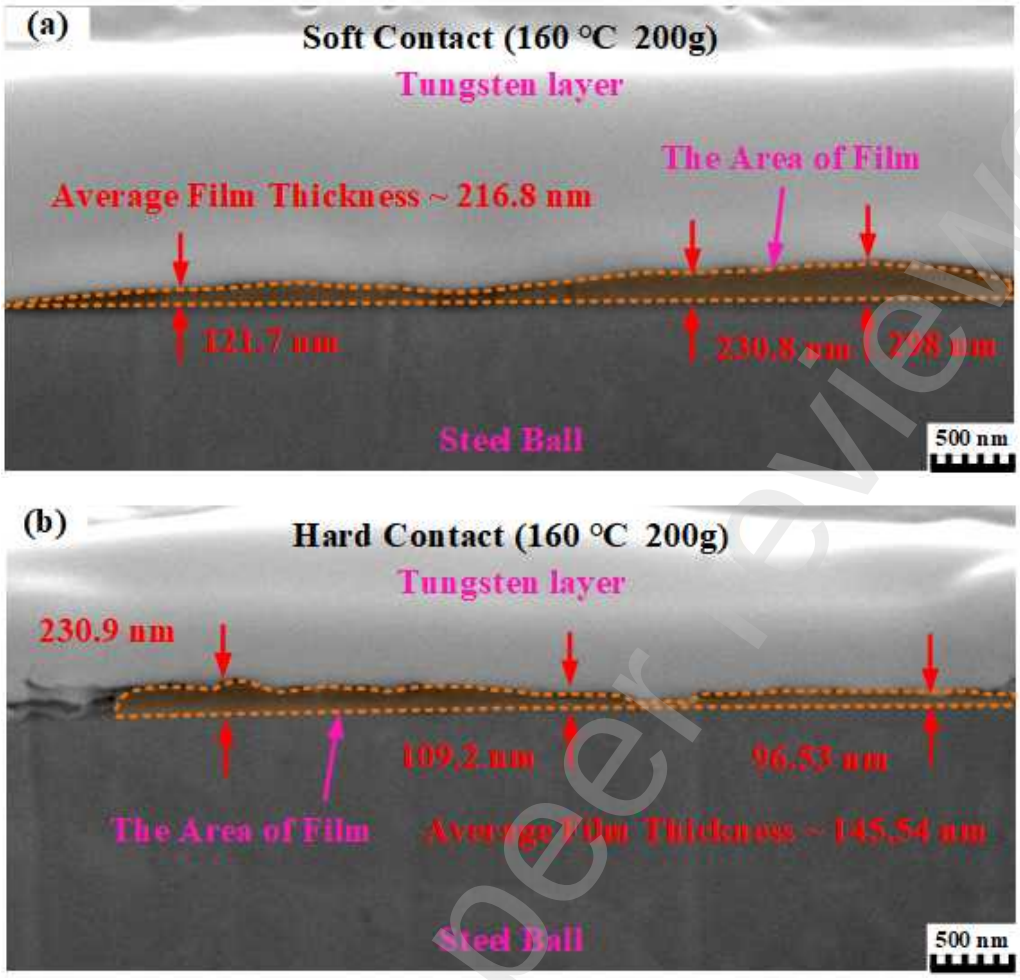

Fig.15 Thickness of ZDDP tribofilms: (a) soft contact, (b) hard contact.

The distribution of the elements on the ZDDP tribofilms were examined by EDS are shown in Fig. 16. EDS line scanning was used to analyze the elemental distribution along the film thickness direction, with the starting point of the scan being the tungsten coating and the endpoint being the steel ball substrate. It can be found that along the film thickness direction, whether under soft contact or hard contact, the element content of Fe consistently increases, while the contents of Zn, P, and S, which are characteristic elements of the ZDDP tribofilms, all decrease. This indicates that the top of the ZDDP tribofilms is enriched with a higher content of Zn. The elemental contents of S and P are comparable but lower than that of Zn.

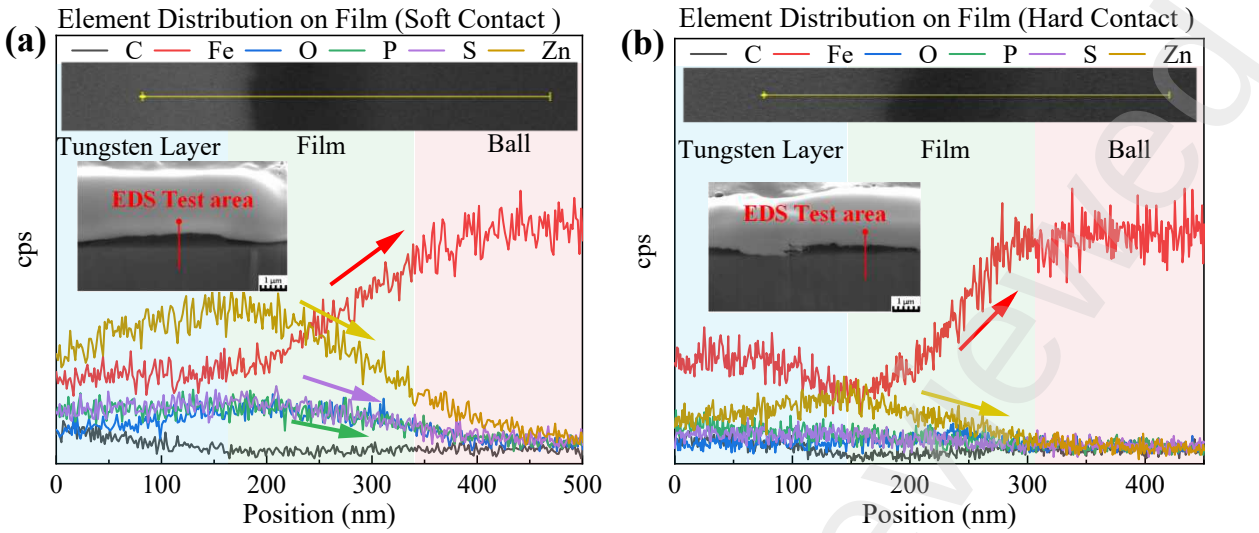

Fig. 16 Distribution of characteristic elements on ZDDP tribofilms: (a) soft contact, (b) hard contact.

Fig. 17 shows the FIB-SEM detection result of no ZDDP tribofilms generated on the surface of the steel ball. It can be observed that the tungsten coating is tightly bonded to the metal substrate, with no gaps between them, indicating that no ZDDP tribofilms are generated on this surface. No Zn or S elements were found in the EDS test results.

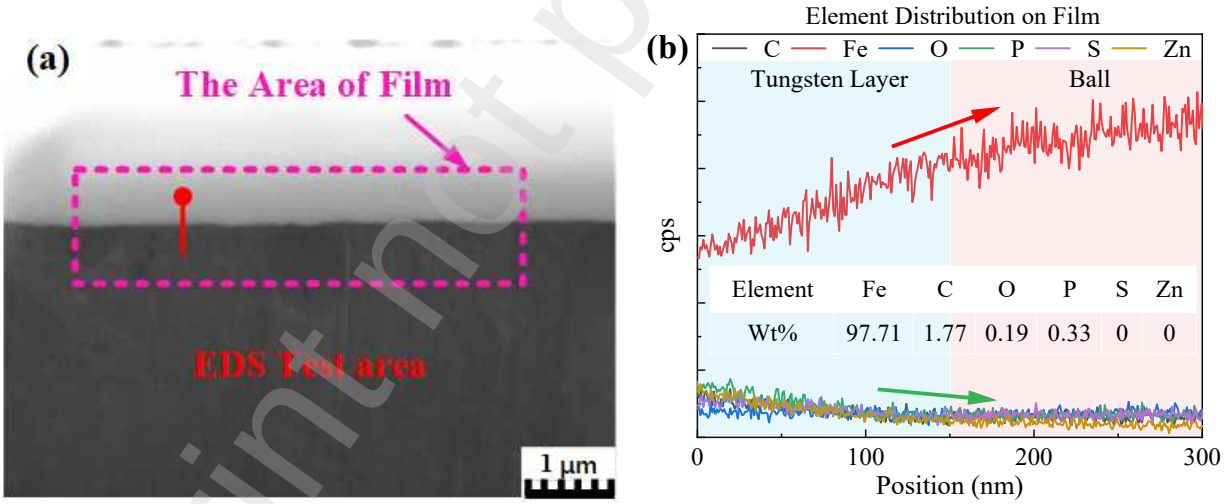

Fig. 17 FIB-SEM testing of steel ball wear surface without generating ZDDP tribofilms: (a) detection area, (b) elements distribution.

3.4 ZDDP tribofilms formation mechanism under soft and hard contact

The formation mechanism of ZDDP tribofilms under soft hard contact is shown in Fig. 18. ZDDP in the lubricating oil forms a protective film on the surface of the worn steel ball through

tribochemistry reactions. Under soft contact, due to the hardness of ZDDP tribofilms (higher than 1.5 GPa) being greater than that of PPI, the wear on the ZDDP tribofilms formed on the surface of the steel ball is less, resulting in a thicker tribofilms (see Fig. 15) and stronger continuity. As the temperature rises, the areas where ZDDP tribofilms on the surface of the steel ball reach their growth limit increase, and the coverage area of ZDDP tribofilms gradually expands. This can aggravate the wear of PPI and even lead to the blackening of the PPI surface (see Fig. 5). In addition, due to the good chemical stability of PPI, ZDDP does not form a film on the worn surface of PPI.

Under hard contact, although ZDDP tribofilms are more likely to form on hard metal substrates, the generated ZDDP tribofilms are also more easily removed by friction due to the higher hardness of the steel disc compared to the ZDDP tribofilms. Therefore, under hard contact, the thickness of ZDDP tribofilms on the worn surface of the steel ball is lower than that under soft contact. Under hard contact, since both the contact surfaces of the steel ball and the steel disc are protected by ZDDP tribofilms, direct contact between the substrates is avoided. Therefore, there is only slight wear on the surfaces of the steel ball and steel disc (at temperature below 120 ℃). At 160 ℃, the viscosity of the lubricating oil significantly decreases, which exacerbates the wear of the steel ball and steel disc.

The Raman spectroscopy detection results on the surface of the steel ball and the elemental distribution on the ZDDP tribofilms indicate that the top of the ZDDP tribofilms is enriched with more Zn. The closer to the substrate, the less Zn content there is. On the substrate surface, S from the thermal decomposition products of ZDDP reacts with the exposed metal, forming a thin layer of iron sulphide. Therefore, the composition of the ZDDP tribofilms can be summarized as follows: a thin layer of iron sulphide forms first on the exposed metal surface, followed by the formation of the main structure of the ZDDP tribofilms, which is a phosphate layer composed of phosphate units. In addition, reference reports have also mentioned that organic ligands can attach to the outermost region of the ZDDP tribofilms.[33]

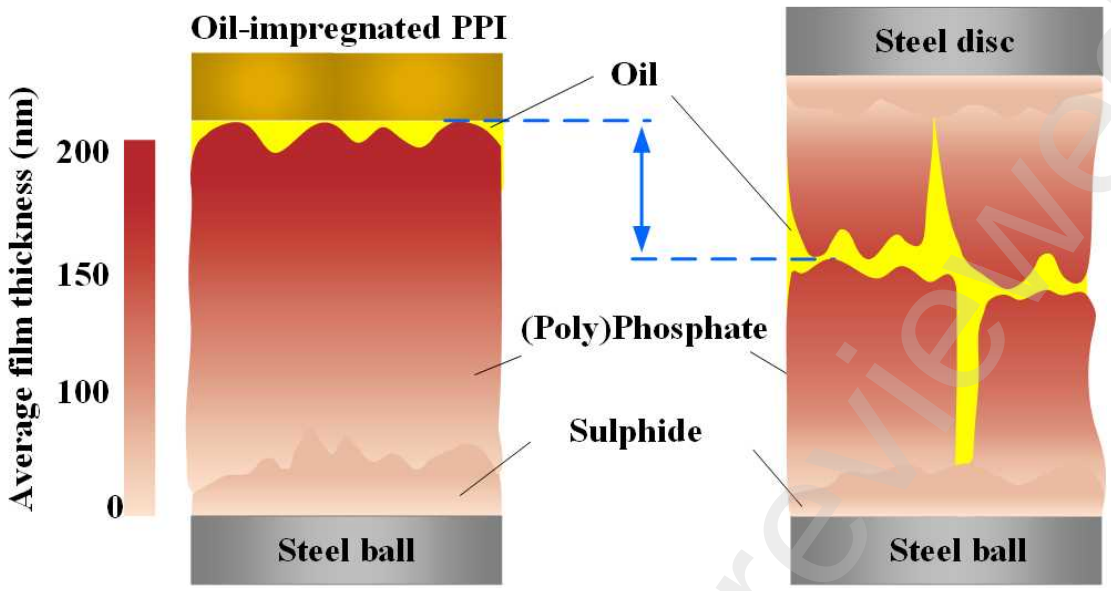

Fig. 18 ZDDP tribofilms formation mechanism under soft and hard contact

4. Conclusions

This article investigates the tribological behavior of ZDDP as a lubricant additive under soft contact (PPI-steel) and hard contact (steel-steel) conditions at different temperatures. The characteristics of ZDDP tribofilms under the two contact types (soft and hard) and their formation mechanisms under these conditions can be summarized as follows:

(1) An increase in temperature promotes the formation of ZDDP tribofilms, which create an anti-wear layer on steel surfaces, thereby reducing wear to the steel substrate. When the temperature is below 80 °C, ZDDP tribofilms provide effective protection for the surfaces of the steel ball and steel disc, preventing severe wear of the PPI surface. Therefore, ZDDP has the potential to be used in bearing lubrication.

(2) Compared with hard contact, the ZDDP tribofilms formed on the surface of the steel ball under soft contact exhibit stronger continuity and greater thickness, thus providing more effective protection.

(3) A thin iron sulphide layer forms at the steel interface as sulfur-containing ZDDP decomposition products react with exposed steel. The main tribofilm develops into a phosphate-rich layer composed of phosphate units, while the outer region is relatively Zn-enriched, with the Zn

content decreasing from the surface toward the substrate.

Acknowledgments

This work was supported by the National Natural Science Foundation of China (U23A20618), Beijing Key Laboratory of Long-life Technology of Precise Rotation and Transmission Mechanisms (No: BZ0388202405), Key Research and Development Program of Ningbo (2025Z133) and the China Scholarship Council (NO: 202509510002).

Appendix A. The curves of friction coefficient under soft and hard contacts

The curves of friction coefficient under soft contact are shown in Fig. A1. It can be seen that the friction curves exhibit more significant fluctuations compared to those under hard contact. This is due to the surface pores of PPI increase the surface roughness. The curves of friction coefficient under hard contact are shown in Fig. A2. The friction coefficient increases rapidly in the initial stage and eventually stabilizes.

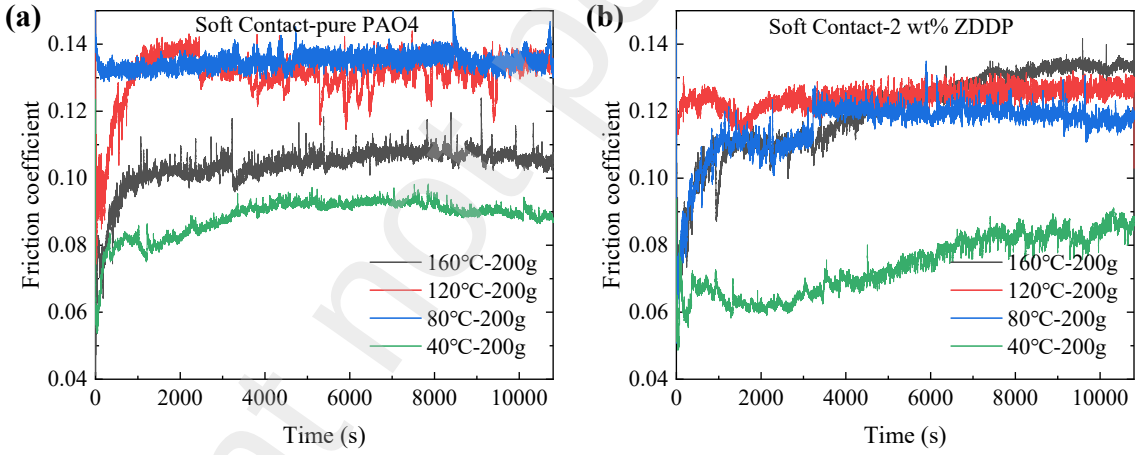

Fig. A1 The curves of friction coefficient: (a) soft contact (pure PAO4), (b) soft contact (2 wt% ZDDP).

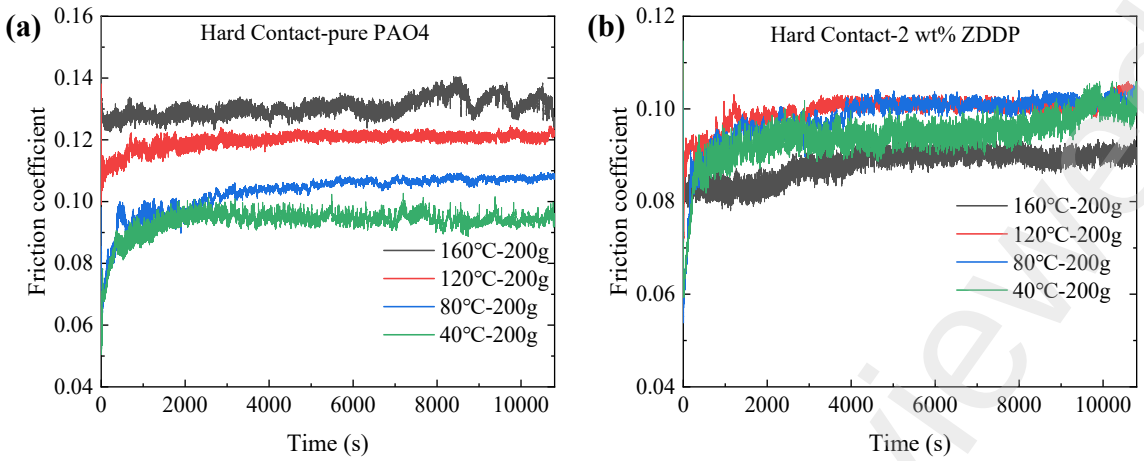

Fig. A2 The curves of friction coefficient: (a) hard contact (pure PAO4), (b) hard contact (2 wt% ZDDP).

Appendix B. Microstructure and elemental maps of worn surfaces on steel ball under hard contact at different temperatures

The generation pattern of the ZDDP tribofilms on the worn surface of steel balls under hard contact is not significantly different from that under soft contact are shown in Fig. B1. The content of characteristic elements on the worn surface of hard contact is shown in Table B1. The distribution pattern of surface elements on steel balls under hard contact is similar to that under soft contact.

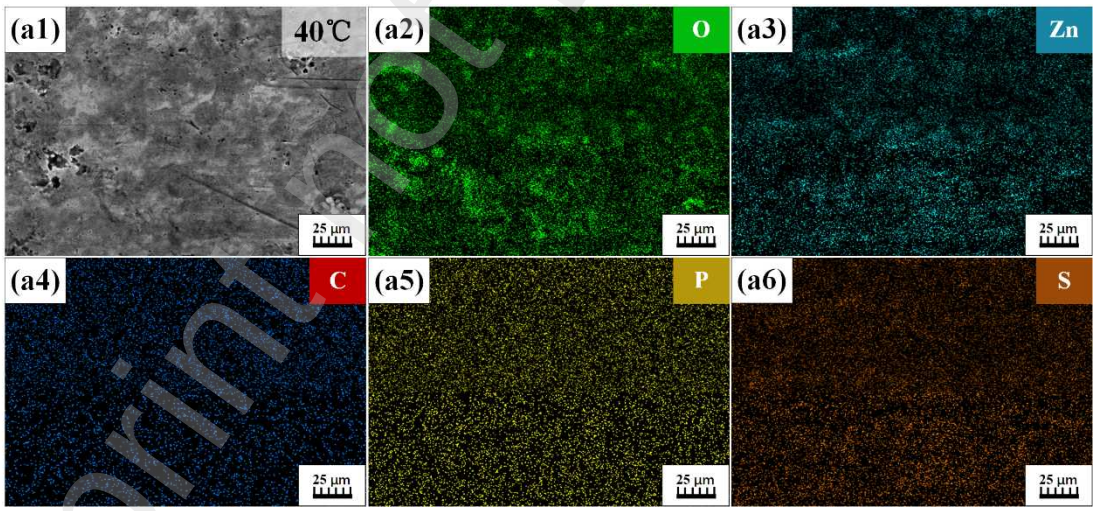

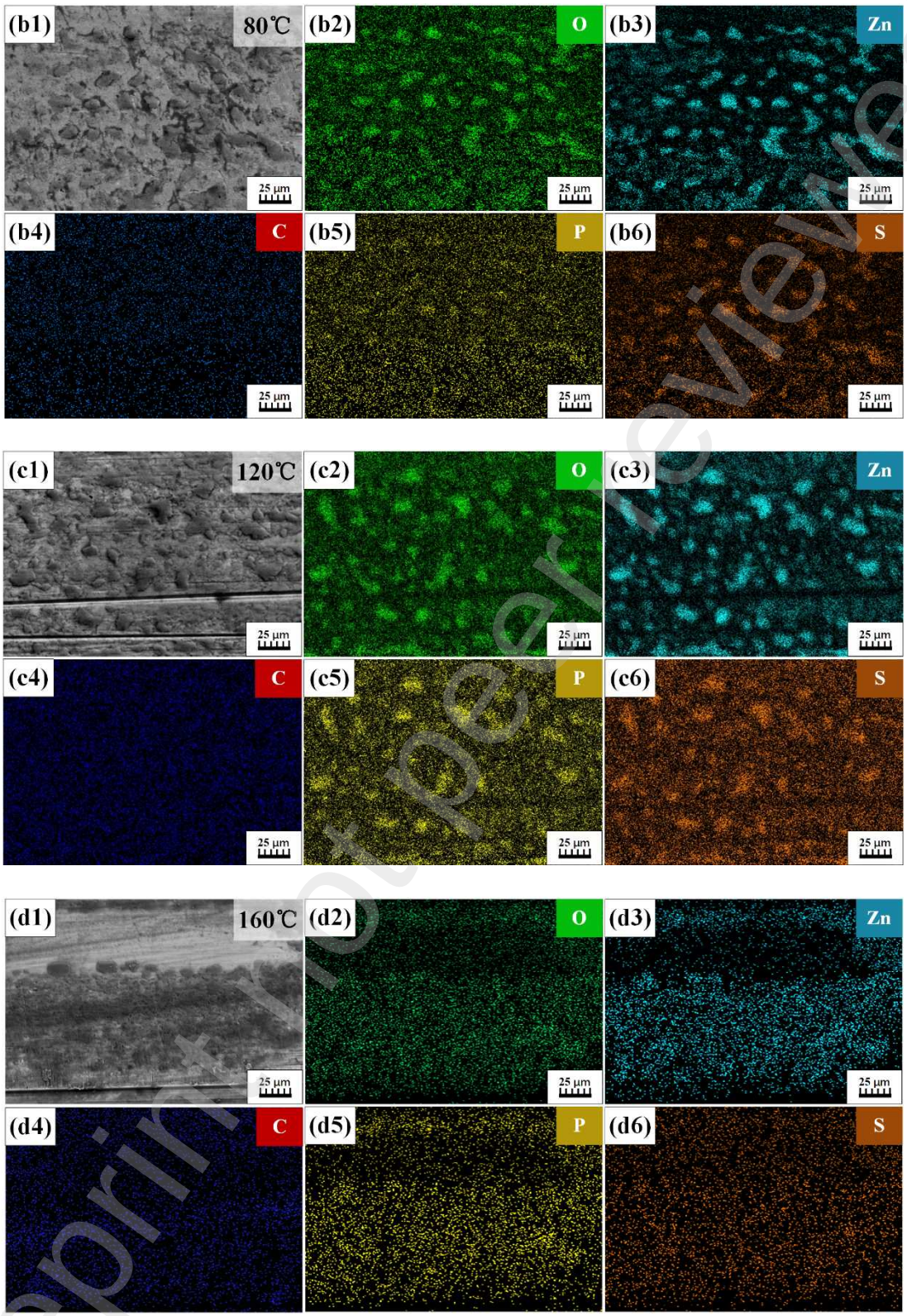

Fig. B1 Microstructure and elemental maps of worn surfaces on steel ball under hard contact at different temperatures: (a1-a6) 40 ℃, (b1-b6) 80 ℃, (c1-c6) 120 ℃, (d1-d6) 160 ℃

Table. B1 The content of characteristic elements on the worn surface of hard contact

Temperature (℃)	Fe (%)	C (%)	O %)	Zn (%)	P (%)	S (%)
40	85.51	5.91	3.32	4.84	0.07	0.35
80	84.21	6.02	2.67	6.17	0.16	0.77
120	80.54	6.58	2.76	8.74	0.7	0.68
160	72.92	6.95	3.15	14.62	1.41	0.95

Appendix C. Random sampling area of FIB-SEM

The sampling area was randomly selected from the worn region on the steel ball surface (at 160 ℃), as shown in Fig. C1. Before sample preparation, a tungsten coating needs to be prepared on the surface of the tribofilm to protect it from damage.

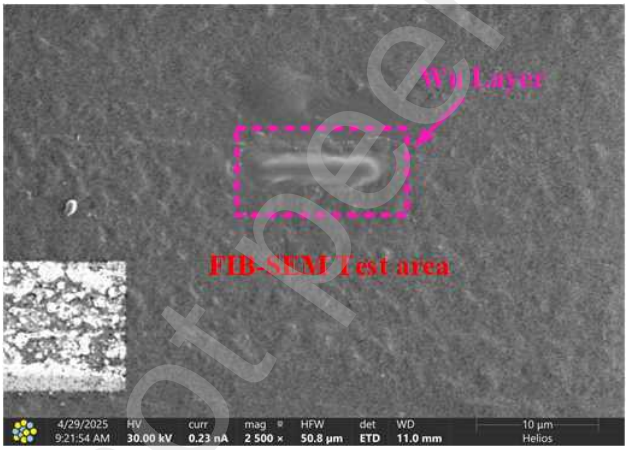

Fig. C1 Sampling area of FIB-SEM

Reference

[1] Wang J, Zhao H, Huang W, Wang X. Investigation of porous polyimide lubricant retainers to improve the performance of rolling bearings under conditions of starved lubrication. Wear. 2017;380-381:52-8. http://doi.org/10.1016/j.wear.2017.03.008

[2] Xu Z, Li J, Li K, Shi C, Zhou N, Hua L, et al. Strengthening Wear Resistance of Porous Polyimide With Organic Silicon Coating. J Appl Polym. 2024;142. http://doi.org/10.1002/app.56597

[3] Chen W, Zhu P, Liang H, Wang W. Characteristic parameter to predict the lubricant outflow from

porous polyimide retainer material. Tribol Int. 2022;173:107596-604. http://doi.org/10.1016/j.triboint.2022.107596

[4] Zhang D, Wang T, Wang Q, Wang C. Selectively enhanced oil retention of porous polyimide bearing materials by direct chemical modification. J Appl Polym. 2017;134:45106-13. http://doi.org/10.1002/app.45106

[5] Gao S, Han Q, Zhou N, Zhang F, Yang Z, Chatterton S, et al. Dynamic and wear characteristics of self-lubricating bearing cage: effects of cage pocket shape. Nonlinear Dynamics. 2022;110:177-200. http://doi.org/10.1007/s11071-022-07611-3

[6] Li J, Liu J, Li K, Zhou N, Liu Y, Hu X, et al. Tribological properties of oil-impregnated polyimide in double-contact friction under micro-oil lubrication conditions. Friction. 2023;11:1493-504. http://doi.org/10.1007/s40544-022-0693-7

[7] Chen W, Wang W, Liang H, Zhu P. Study on Lubricant Release-Recycle Performance of Porous Polyimide Retainer Materials. Langmuir. 2022;38:11440-50. http://doi.org/10.1021/acs.langmuir.2c01781

[8] Bertrand PA, Carré DJ. Oil Exchange between Ball Bearings and Porous Polyimide Ball Bearing Retainers. Tribol Trans. 1997;40:294-302. http://doi.org/10.1080/10402009708983658

[9] Yin Y, Shi P, Zhang S, Jiang Y, Qing T, Wang Y, et al. Improving Tribological Performance of Porous Polyimide by Surface Polishing. ACS Appl Polyme. 2023;5:6808-16. http://doi.org/10.1021/acsapm.3c00795

[10] Jia W, Yang S, Ren S, Ma L, Wang J. Preparation and tribological behaviors of porous oil-containing polyimide/hollow mesoporous silica nanospheres composite films. Tribol Int. 2020;145:106184-92. http://doi.org/10.1016/j.triboint.2020.106184

[11] Cheng Y, Wang Y, Lin J, Xu S, Zhang P. Research status of the influence of machining processes and surface modification technology on the surface integrity of bearing steel materials. The International Journal of Advanced Manufacturing Technology. 2023;125:2897-923. http://doi.org/10.1007/s00170-023-10960-x

[12] Cheng Y, Wang Y, Wang Z, Huang P, Zhang P, Guo Q. Ultrasonic surface rolling strengthening and its parameter optimization on bearing raceway. Materials & Design. 2023;232:112156. http://doi.org/https://doi.org/10.1016/j.matdes.2023.112156

[13] Cao Z, Liu T, Yu F, Cao W, Zhang X, Weng Y. Carburization induced extra-long rolling contact

fatigue life of high carbon bearing steel. Int J Fatigue. 2020;131:105351. http://doi.org/https://doi.org/10.1016/j.ijfatigue.2019.105351

[14] Saied C, Chala A, Belahssen O, Benramache S. TRIBOLOGICAL BEHAVIOR OF 42CrMo4 STEEL NITRIDED BY PLASMA. Acta Metallurgica Slovaca. 2015;21:220-5. http://doi.org/10.12776/ams.v21i3.563

[15] Zhao X, Wang B, Sun D, Li C, Han L, Gu J. Effect of pre-existing VC carbides on nitriding and wear behavior of hot-work die steel. Applied Surface Science. 2019;486:179-86. http://doi.org/https://doi.org/10.1016/j.apsusc.2019.04.270

[16] Lin Y, He R, Xu Y, Zhang J, Wetzel B, Zhang G. Significance of nickel particles on reducing friction and wear of polyimide subjected to harsh boundary lubrication conditions. Tribol Int. 2023;178:108063-74. http://doi.org/10.1016/j.triboint.2022.108063

[17] Xie X, Chen C, Luo J, Xu J. The microstructure and tribological properties of M50 steel surface after titanium ion implantation. Applied Surface Science. 2021;564:150349. http://doi.org/https://doi.org/10.1016/j.apsusc.2021.150349

[18] Wang F, Zhou C, Zheng L, Zhang H. Corrosion resistance of carbon ion-implanted M50NiL aerospace bearing steel. Progress in Natural Science: Materials International. 2017;27:615-21. http://doi.org/https://doi.org/10.1016/j.pnsc.2017.07.003

[19] Jin F, Chu PK, Xu Z, Zhao J, Zhu M, Fu RKY, et al. Surface modification of W9Cr4V2Mo high-temperature bearing steel by rare earth ion implantation. Surf Coat Technol. 2006;201:4357-60. http://doi.org/https://doi.org/10.1016/j.surfcoat.2006.08.064

[20] Jin J, Chen Y, Gao K, Huang X. The effect of ion implantation on tribology and hot rolling contact fatigue of Cr4Mo4Ni4V bearing steel. Applied Surface Science. 2014;305:93-100. http://doi.org/https://doi.org/10.1016/j.apsusc.2014.02.174

[21] Zhao Y, Geng Z, Li D, Wang L, Lu Z, Zhang G. An investigation on the tribological properties of graphene and ZDDP as additives in PAO4 oil. Diamond Relat Mater. 2021;120:108635. http://doi.org/https://doi.org/10.1016/j.diamond.2021.108635

[22] Zhang J, Spikes H. On the Mechanism of ZDDP Antiwear Film Formation. Tribol Lett. 2016;63:24. http://doi.org/10.1007/s11249-016-0706-7

[23] Spikes H. The History and Mechanisms of ZDDP. Tribol Lett. 2004;17:469-89. http://doi.org/10.1023/B:TRIL.0000044495.26882.b5

[24] Fujita H, Spikes HA. The formation of zinc dithiophosphate antiwear films. Proceedings of the Institution of Mechanical Engineers, Part J: Journal of Engineering Tribology. 2004;218:265-78. http://doi.org/10.1243/1350650041762677

[25] Zhang J, Ueda M, Campen S, Spikes H. Boundary Friction of ZDDP Tribofilms. Tribol Lett. 2020;69. http://doi.org/10.1007/s11249-020-01389-4

[26] Zhang J, Ewen JP, Ueda M, Wong JSS, Spikes HA. Mechanochemistry of Zinc Dialkyldithiophosphate on Steel Surfaces under Elastohydrodynamic Lubrication Conditions. ACS Appl Mater. 2020;12:6662-76. http://doi.org/10.1021/acsami.9b20059

[27] Onodera T, Kuriaki T, Morita Y, Suzuki A, Koyama M, Tsuboi H, et al. Influence of nanometer scale film structure of ZDDP tribofilm on Its mechanical properties: A computational chemistry study. Applied Surface Science. 2009;256:976-9. http://doi.org/https://doi.org/10.1016/j.apsusc.2009.04.205

[28] Bartolomé L, Oblak E, Kalin M. Mechanical behaviour and constitutive models of ZDDP tribofilms on DLC coatings using nano-indentation data and finite element modelling. Tribol Int. 2016;95:19-26. http://doi.org/10.1016/j.triboint.2015.10.036

[29] Fang L, Korres S, Lamberti WA, Webster Martin N, Carpick RW. What stress components drive mechanochemistry? A study of ZDDP tribofilm formation. Faraday Discuss. 2023;241:394-412. http://doi.org/10.1039/d2fd00123c

[30] Graham JF, McCague C, Norton PR. Topography and nanomechanical properties of tribochemical films derived from zinc dialkyl and diaryl dithiophosphates. Tribol Lett. 1999;6:149-57. http://doi.org/10.1023/A:1019124026402

[31] Li J, Yang Q, Xu Z, Zhao J, Shi C, Zhou N, et al. Tribofilm Formation of Zinc Dialkyldithiophosphate as Oil Additives Impregnated in Porous Polyimide under Different Contacts. Langmuir. 2024;40:9439-48. http://doi.org/10.1021/acs.langmuir.3c03849

[32] D. Botto, M. Lavella. High temperature tribological study of cobalt-based coatings reinforced with different percentages of alumina. Tribol Int. 2014;318:89-97. https://doi.org/10.1016/j.wear.2014.06.024

[33] Anderluh R, Al-Sallami W, Anderson W, Jasak H. Accounting for mechanical properties of ZDDP tribofilms in continuum-based wear simulations. Tribol Int. 2025;208. http://doi.org/10.1016/j.triboint.2025.110639

[34] Bec S, Tonck A, Georges J-M, Coy RC, Bell JC, Roper GWJPotRSoLSAM, Physical, et al. Relationship between mechanical properties and structures of zinc dithiophosphate anti–wear films. 1999;455:4181-203. https://doi.org/10.1098/rspa.1999.0497

[35] Bell J, Delargy K. . Proceeding of the 6th International Congress on Tribology1993. p. 328-32.

[36] Garcia CE, Ueda M, Spikes H, Wong JSS. Temperature dependence of molybdenum dialkyl dithiocarbamate (MoDTC) tribofilms via time-resolved Raman spectroscopy. Scientific Reports. 2021;11. http://doi.org/10.1038/s41598-021-81326-0

[37] B. Hamrock DD. Isothermal Elastohydrodynamic Lubrication of Point Contacts: Part III-fully Flooded Results. Journal of Lubrication Technology. 1977:264-75. https://doi.org/10.1115/1.3453074

[38] Zhang J, Campen S, Wong J, Spikes H. Oxidational wear in lubricated contacts – Or is it? Tribol Int. 2022;165. http://doi.org/10.1016/j.triboint.2021.107287

[39] Taeño M, Torre F, Huerta-Flores AM, Luengo C, Azpiazu A, Del Barrio EP, et al. Microwave-induced hydrogen production at medium temperature of iron oxide/hercynite composite. Int J Hydrogen Energy. 2025;97:718-26. http://doi.org/10.1016/j.ijhydene.2024.11.476

[40] Demmou K, Bec S, Loubet J-L, Martin J-M. Temperature effects on mechanical properties of zinc dithiophosphate tribofilms. Tribol Int. 2006;39:1558-63. http://doi.org/https://doi.org/10.1016/j.triboint.2006.01.025

[41] Feng W, Song H, Lu Z, ZhiquanYang, Hu X. On the mechanical and tribological performances of the tribofilm formed by zinc dialkyl dithiophosphate. Journal of Industrial and Engineering Chemistry. 2023;122:152-60. http://doi.org/10.1016/j.jiec.2023.02.017

[42] Ferrari AC, Robertson J. Interpretation of Raman spectra of disordered and amorphous carbon. Physical Review B. 2000;61:14095-107. http://doi.org/10.1103/PhysRevB.61.14095

[43] Shi P, Yin Y, Zhang S, Zhang D, Jiang Y, Wang Y, et al. Blackening failure of poly-α-olefin impregnated porous polymide due to the splitting of lubrication oil catalyzed by iron. Friction. 2024. http://doi.org/10.1007/s40544-023-0829-4

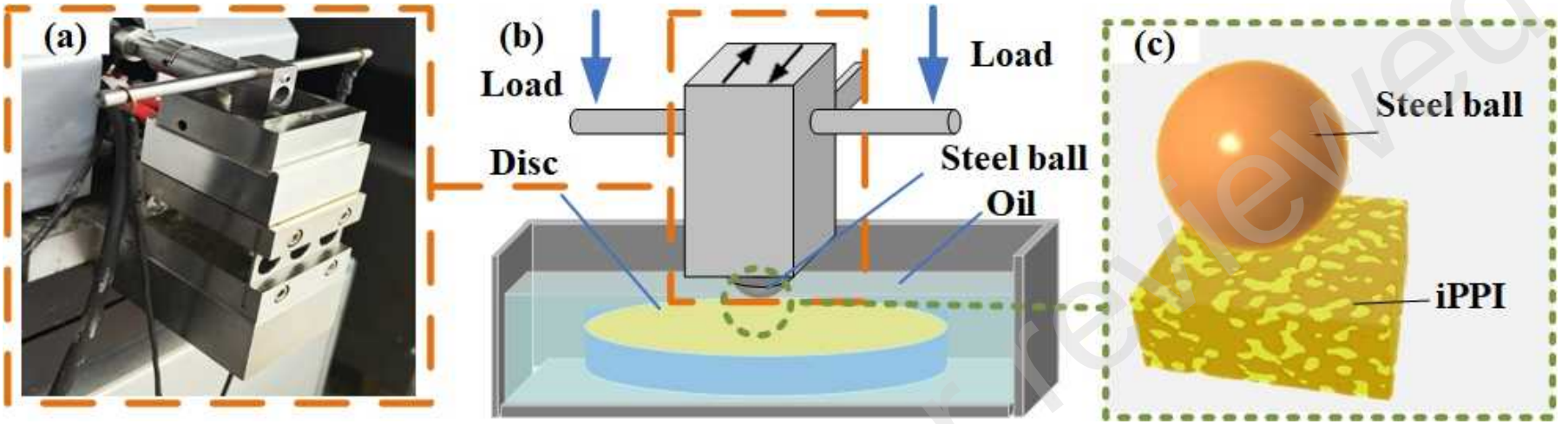

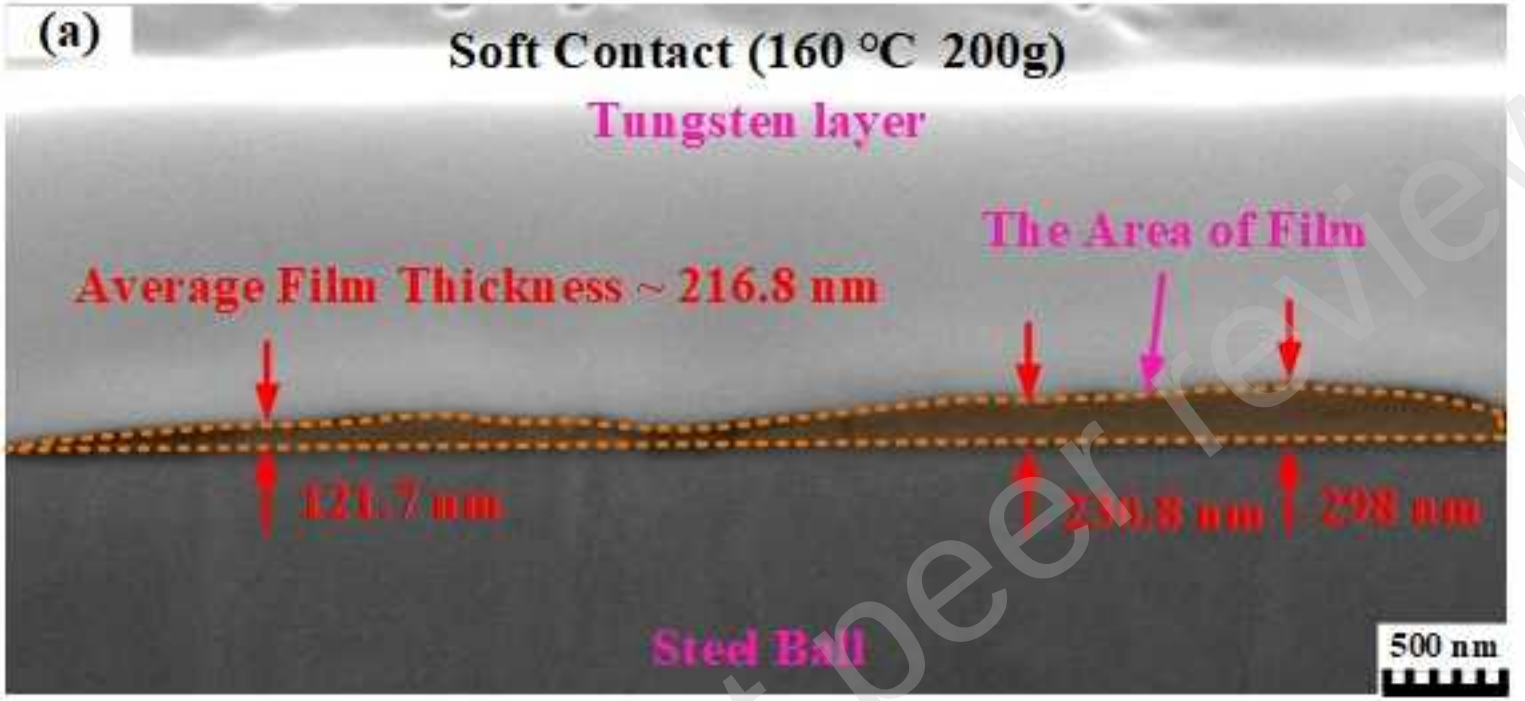

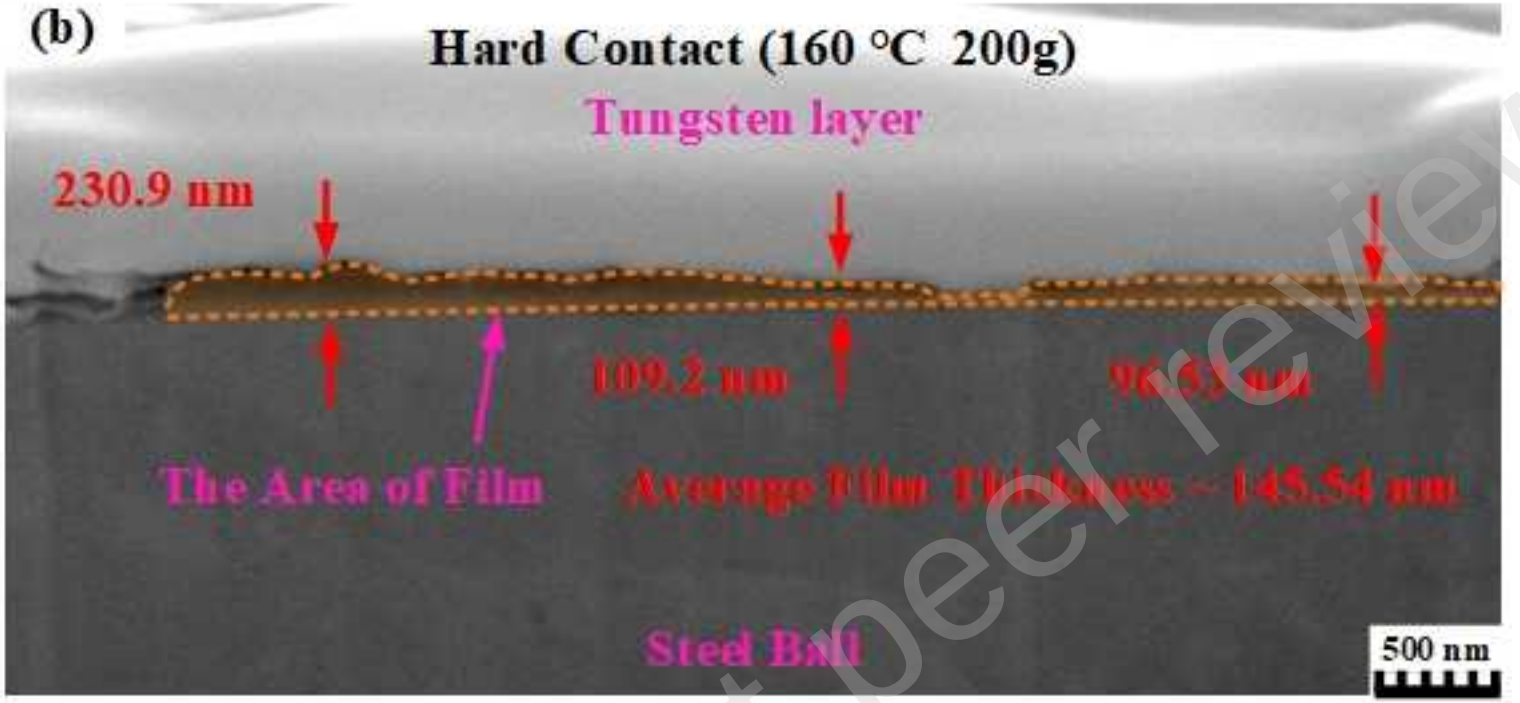

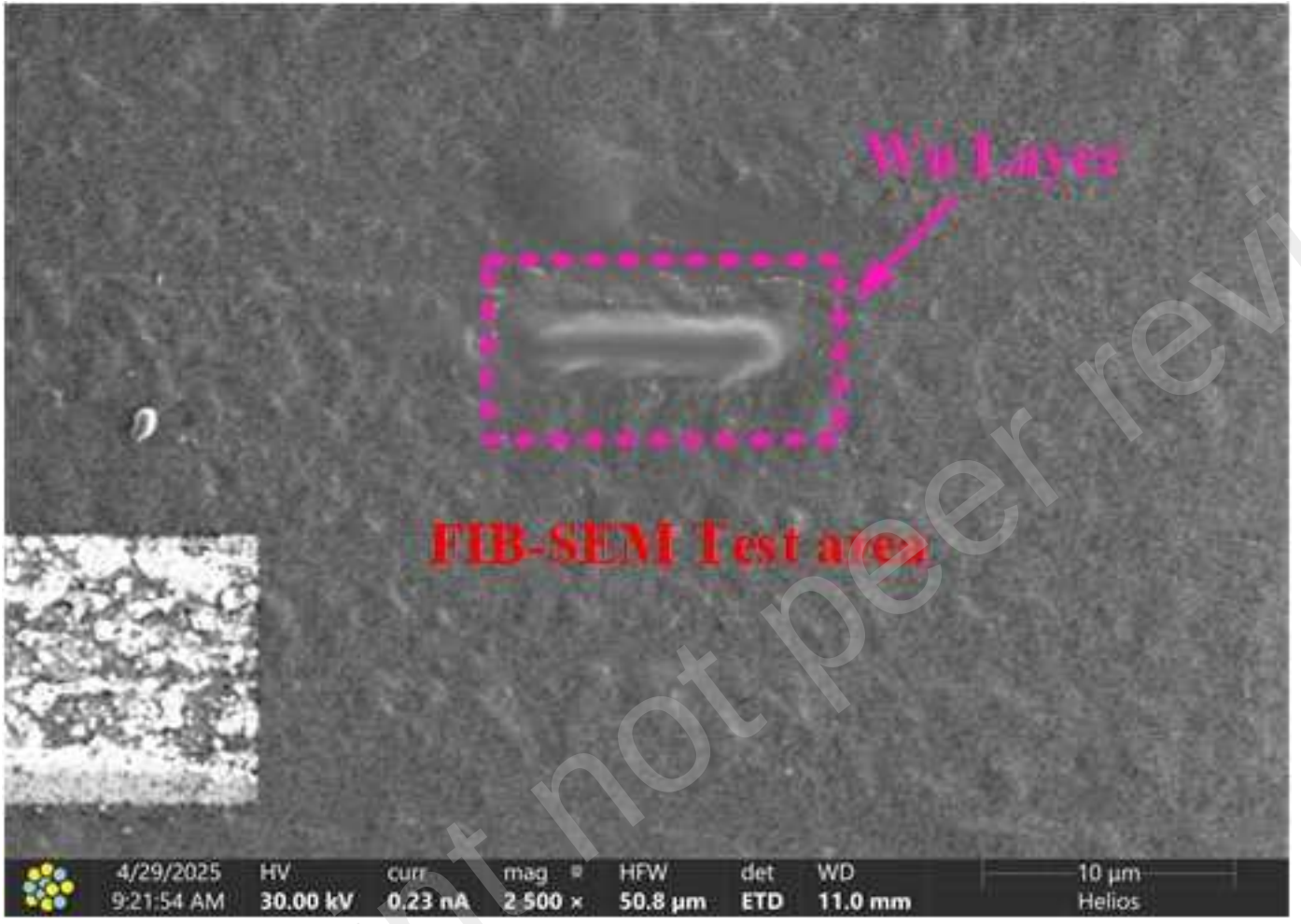

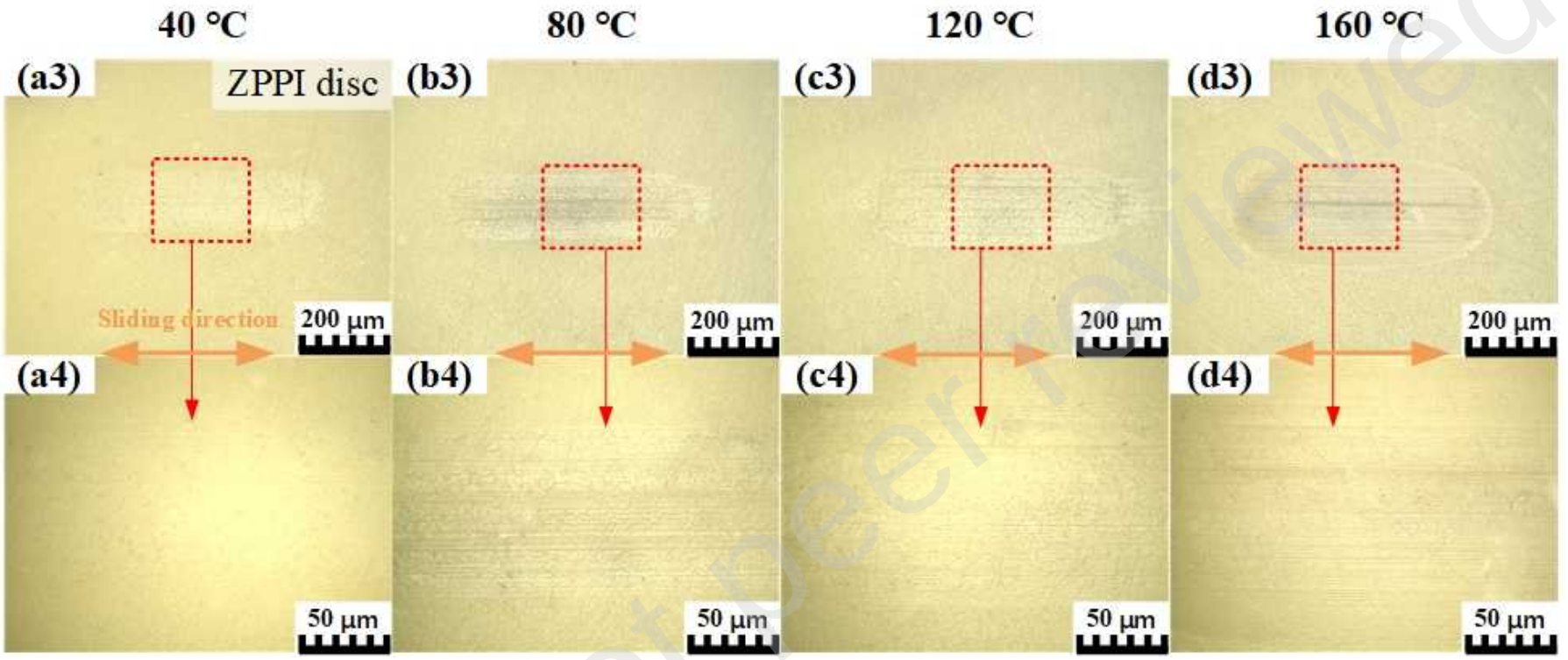

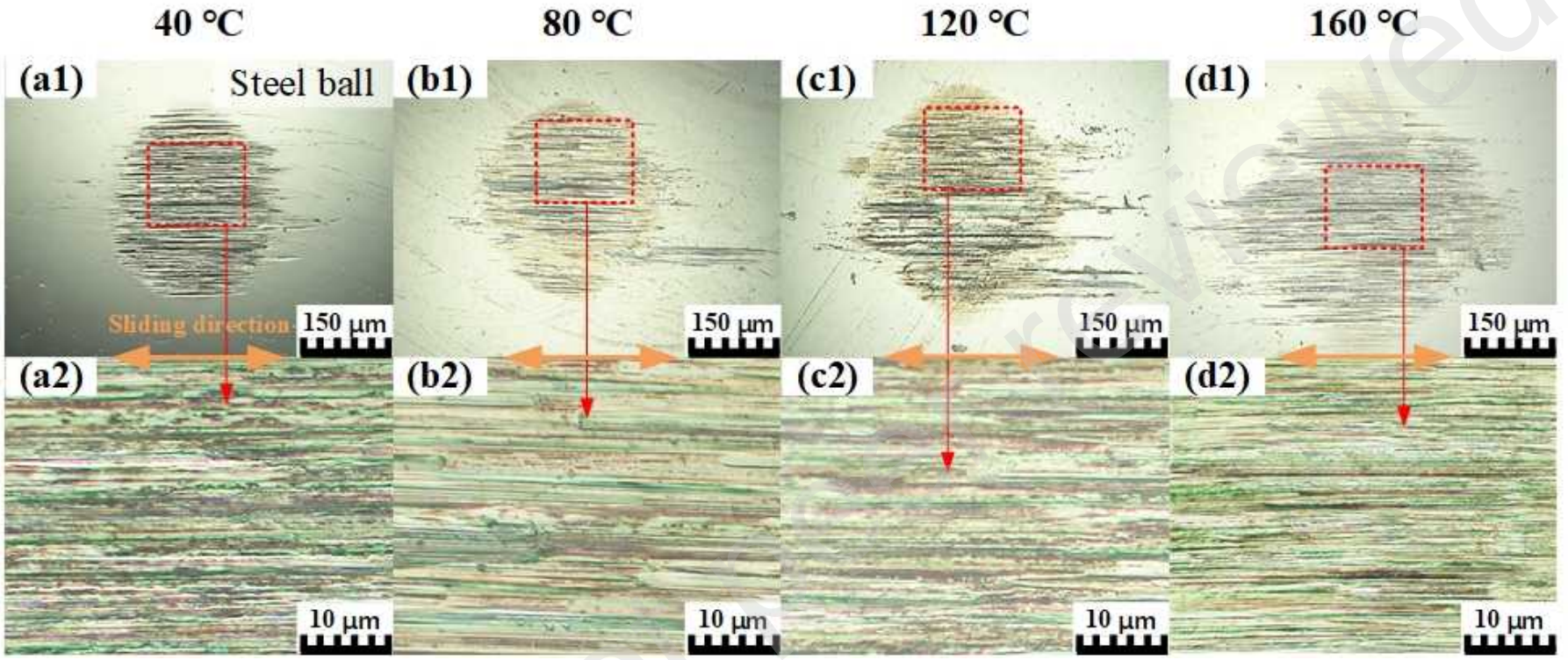

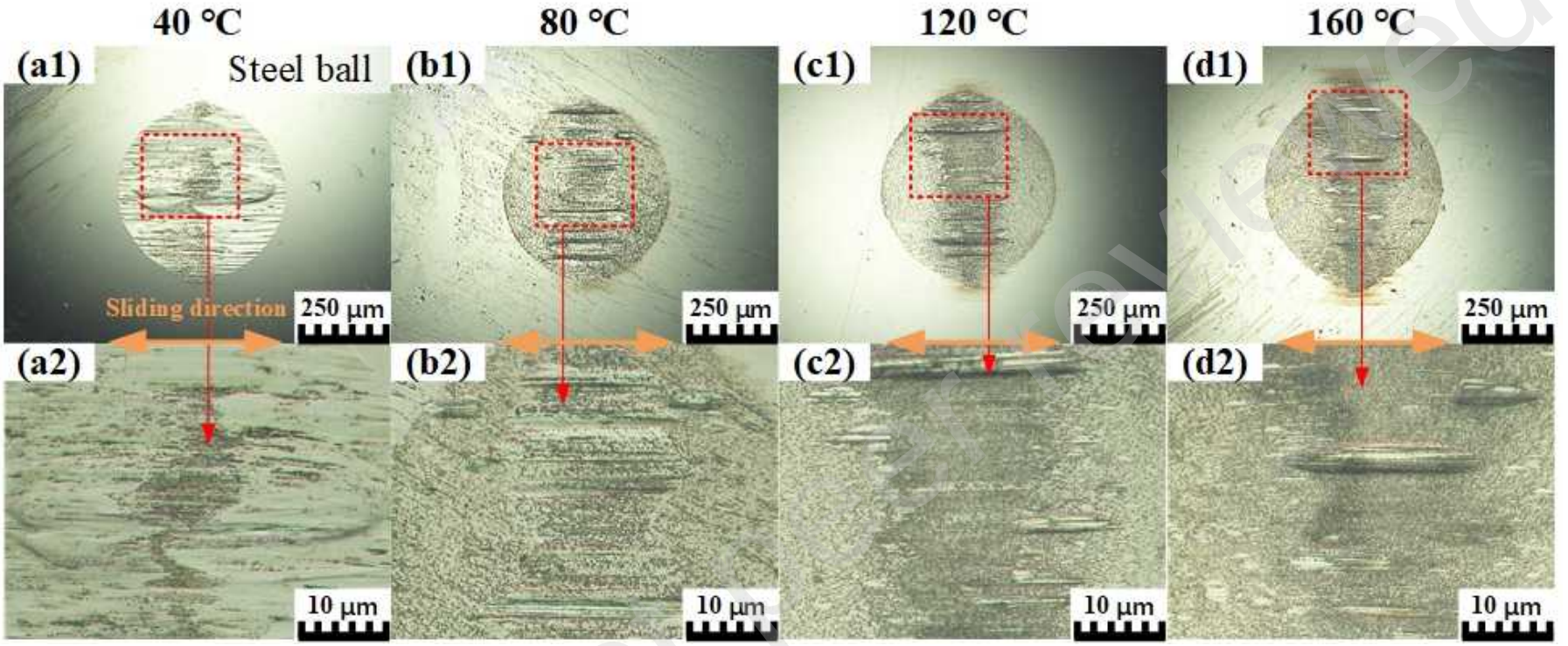

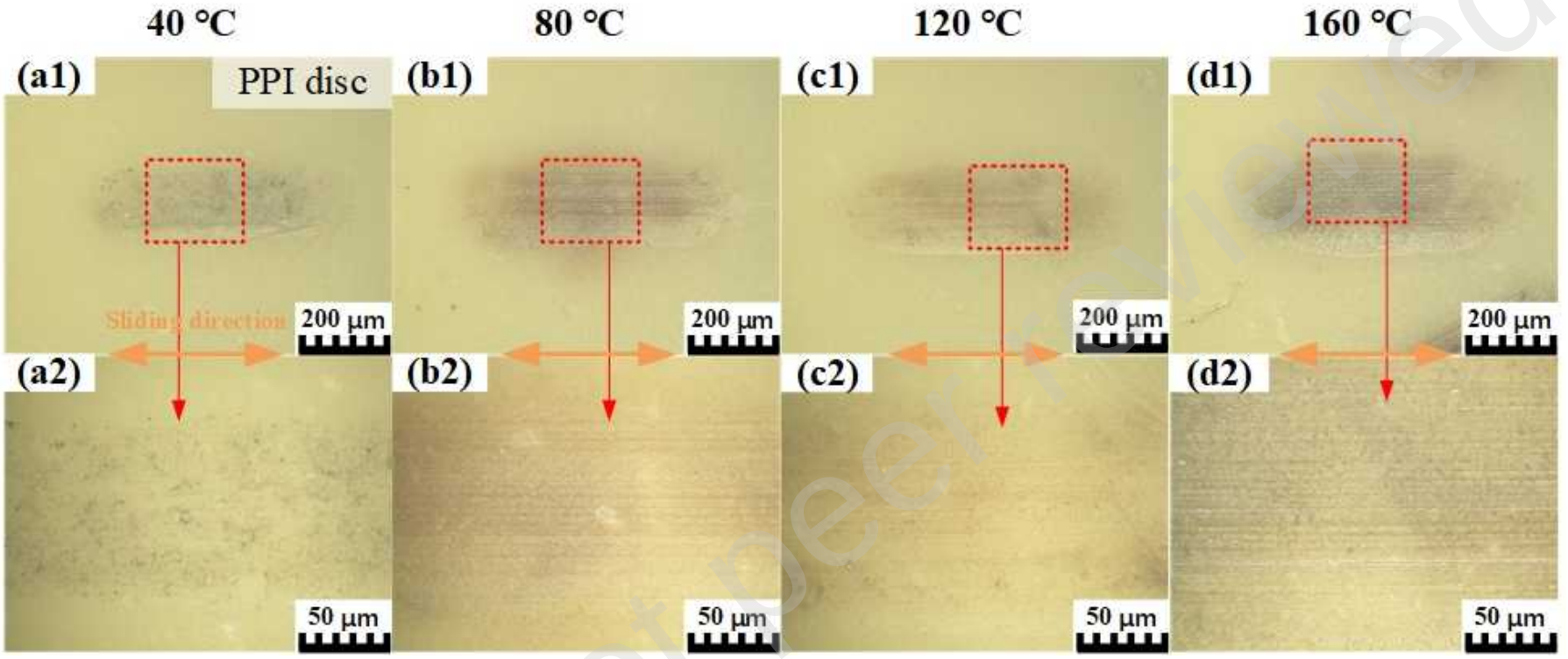

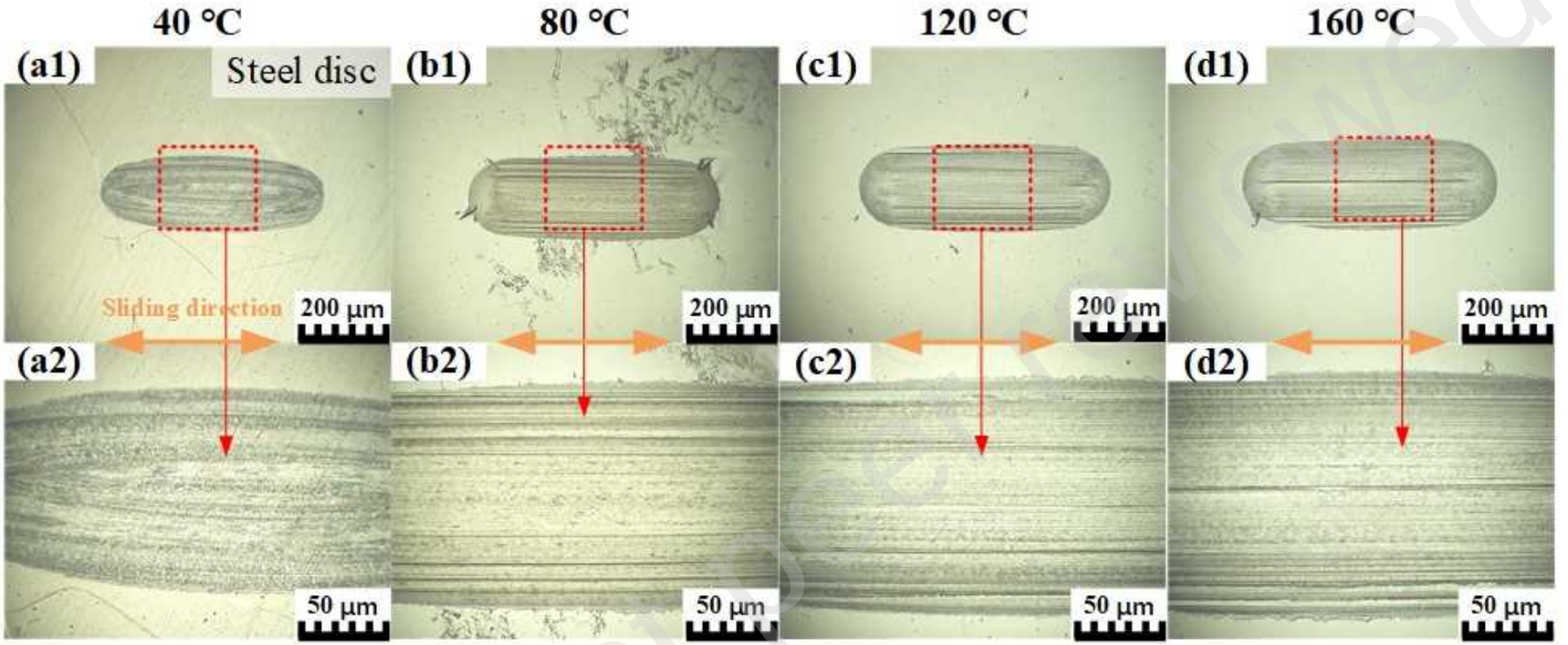

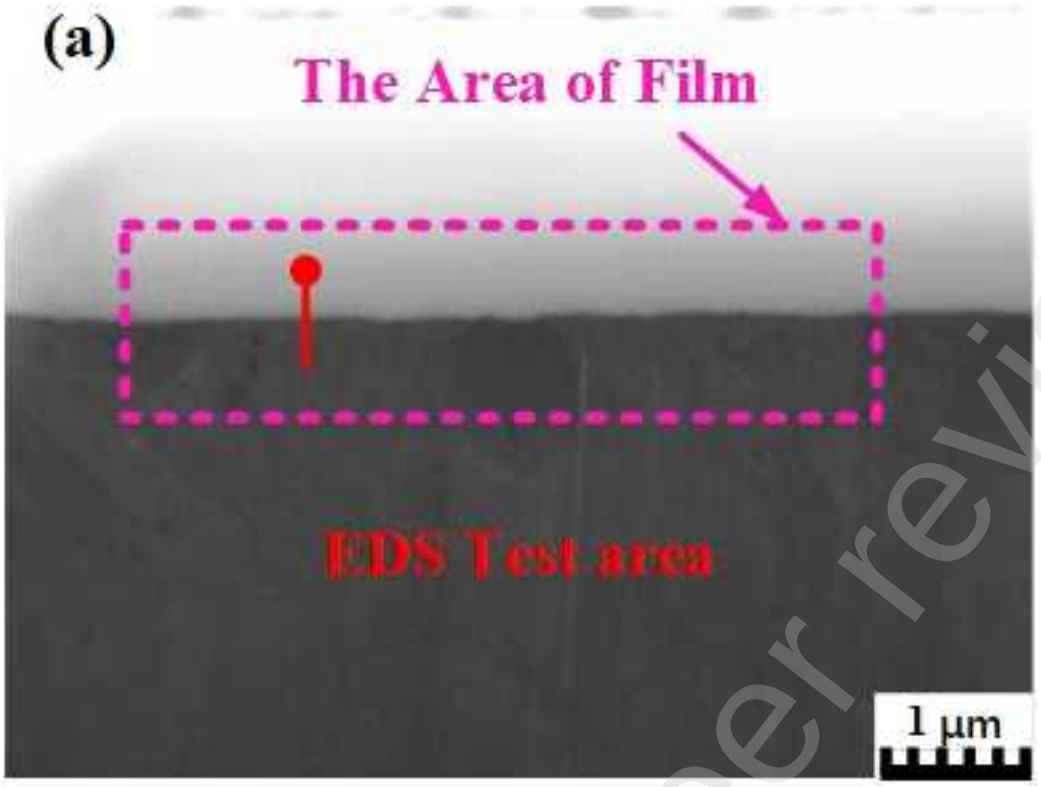

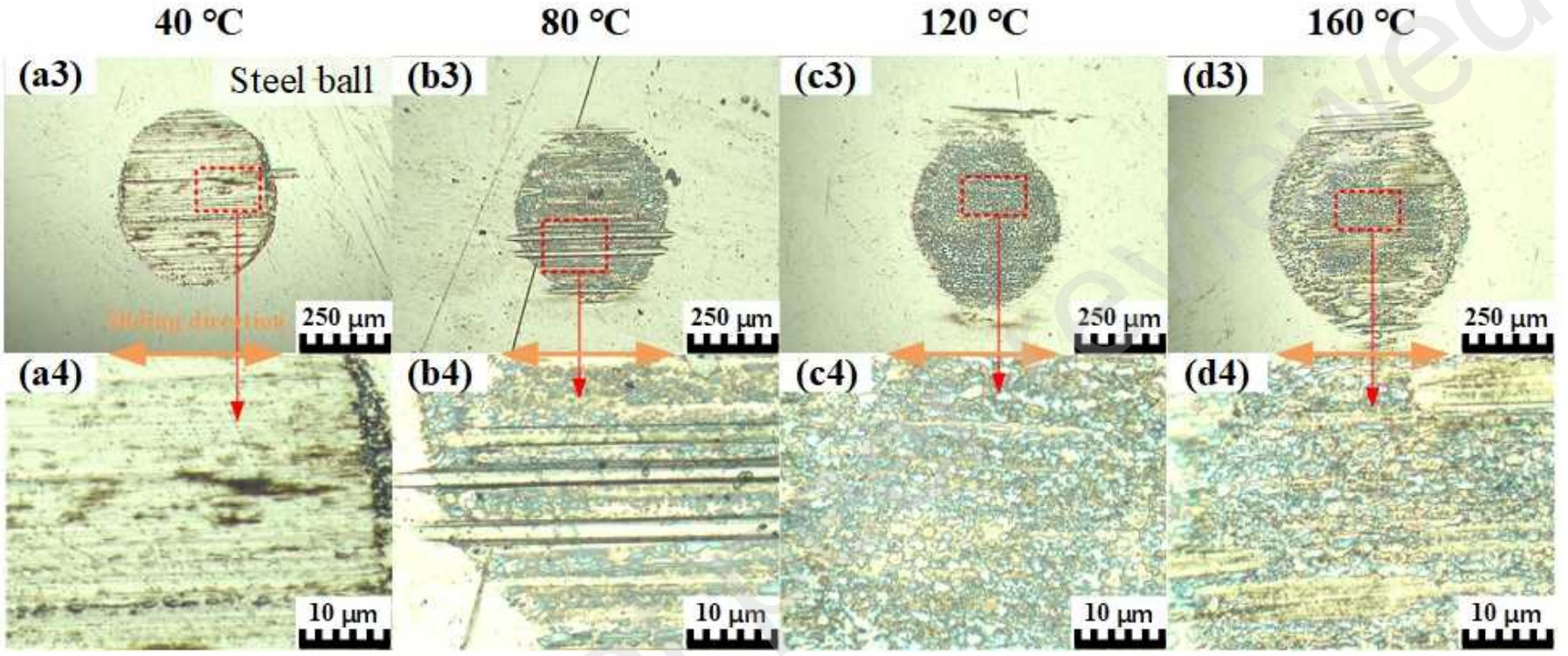

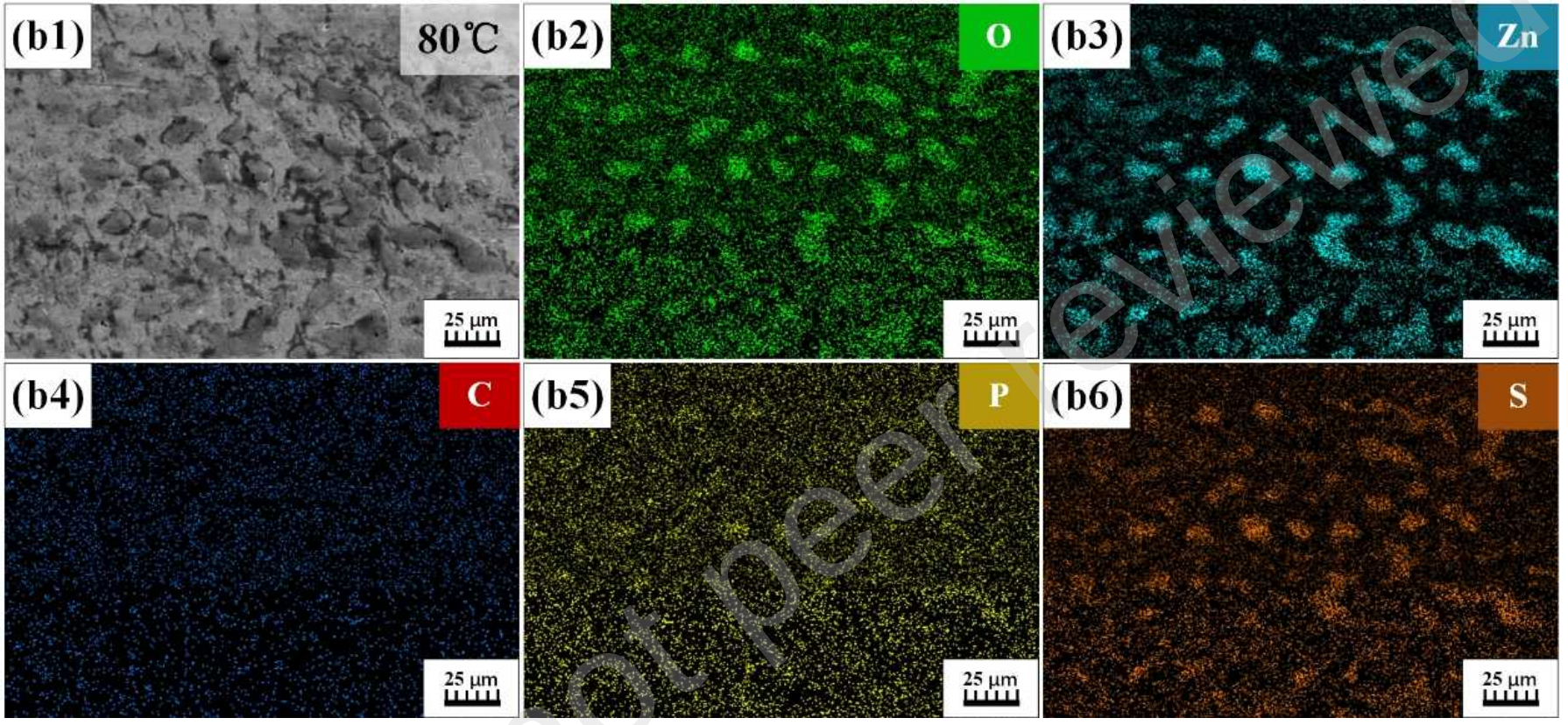

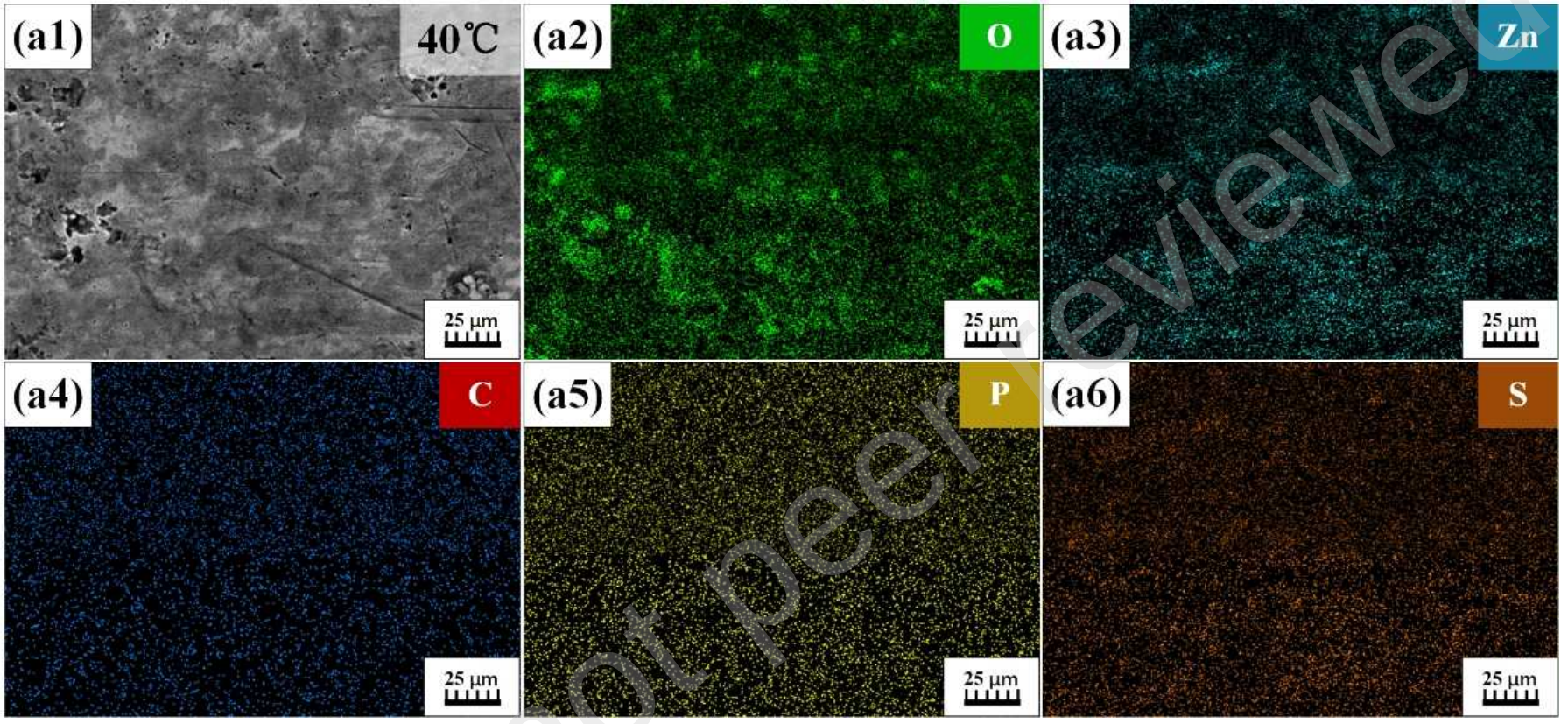

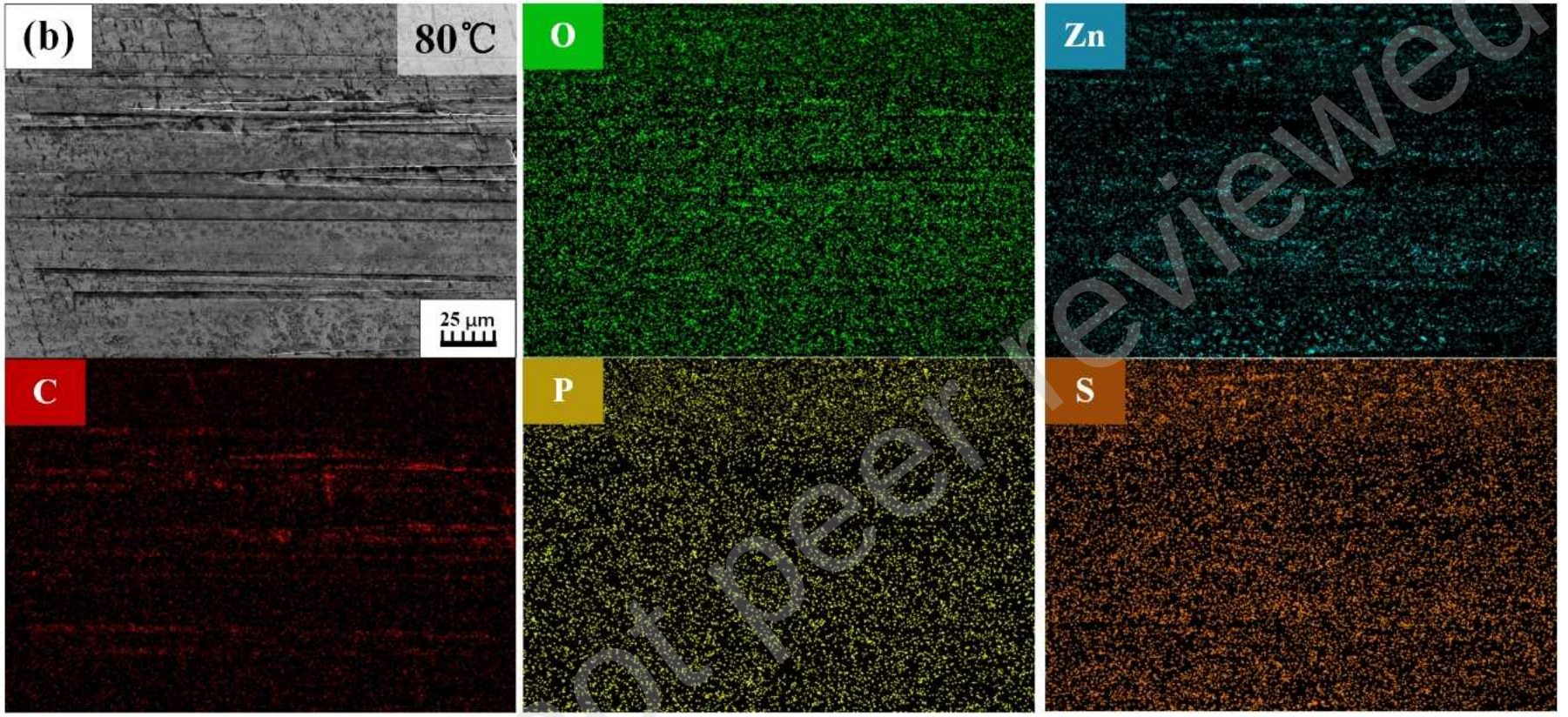

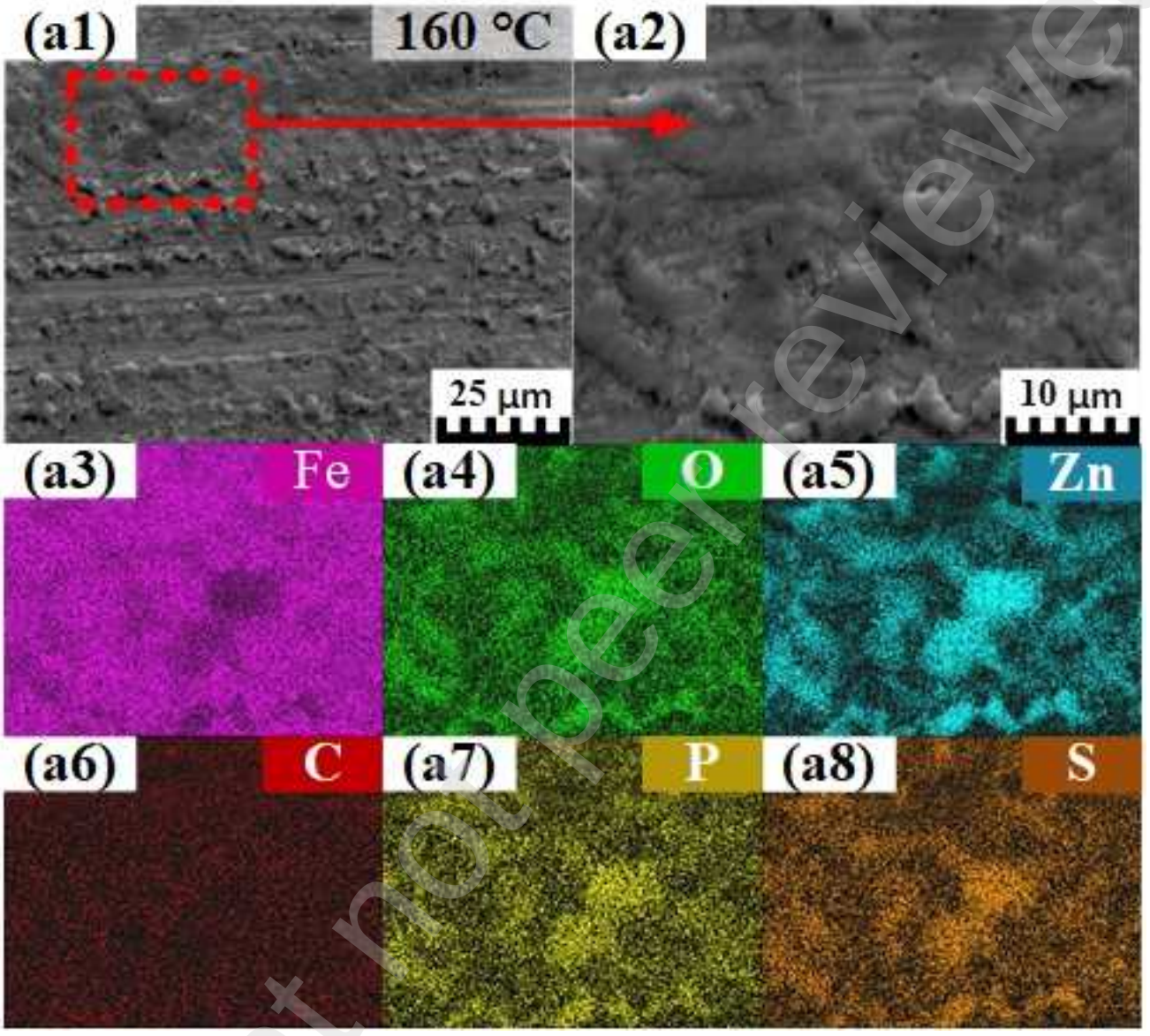

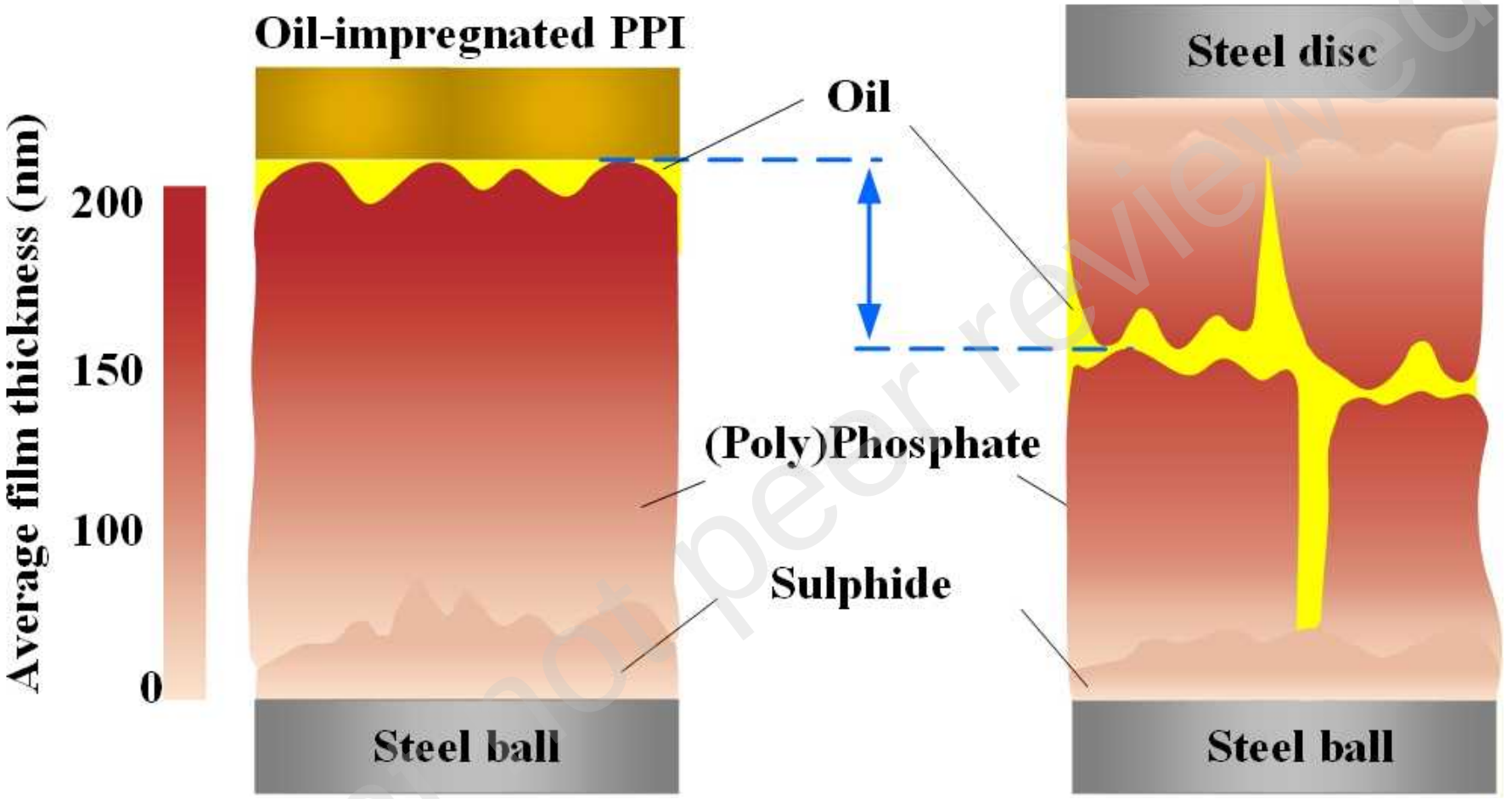

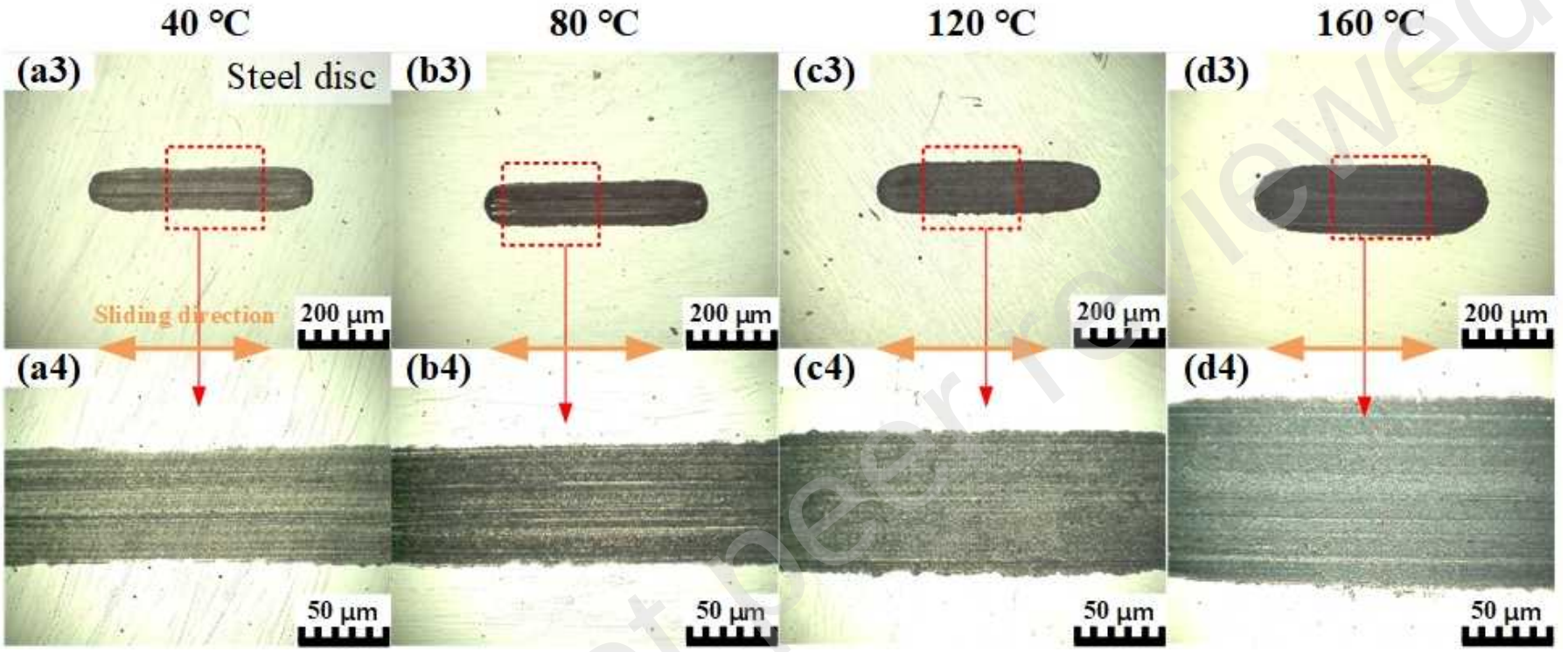

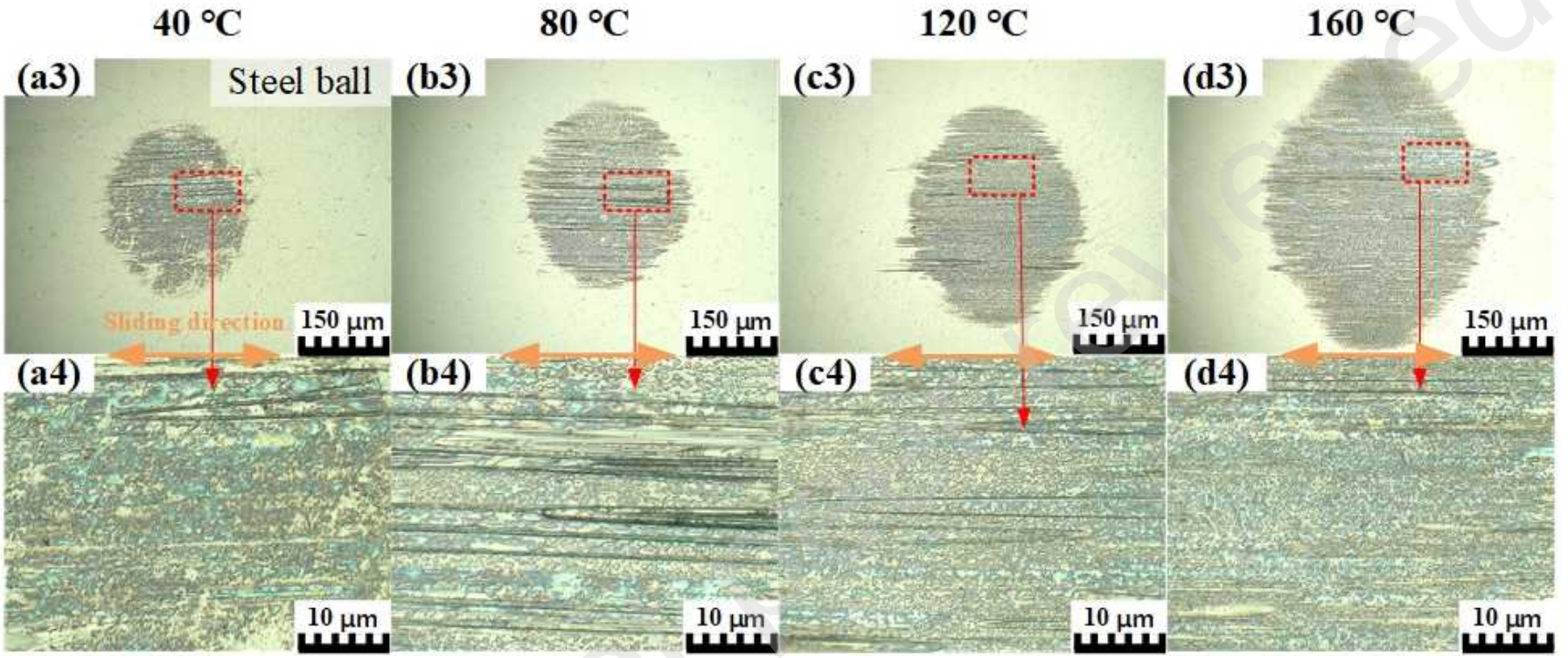

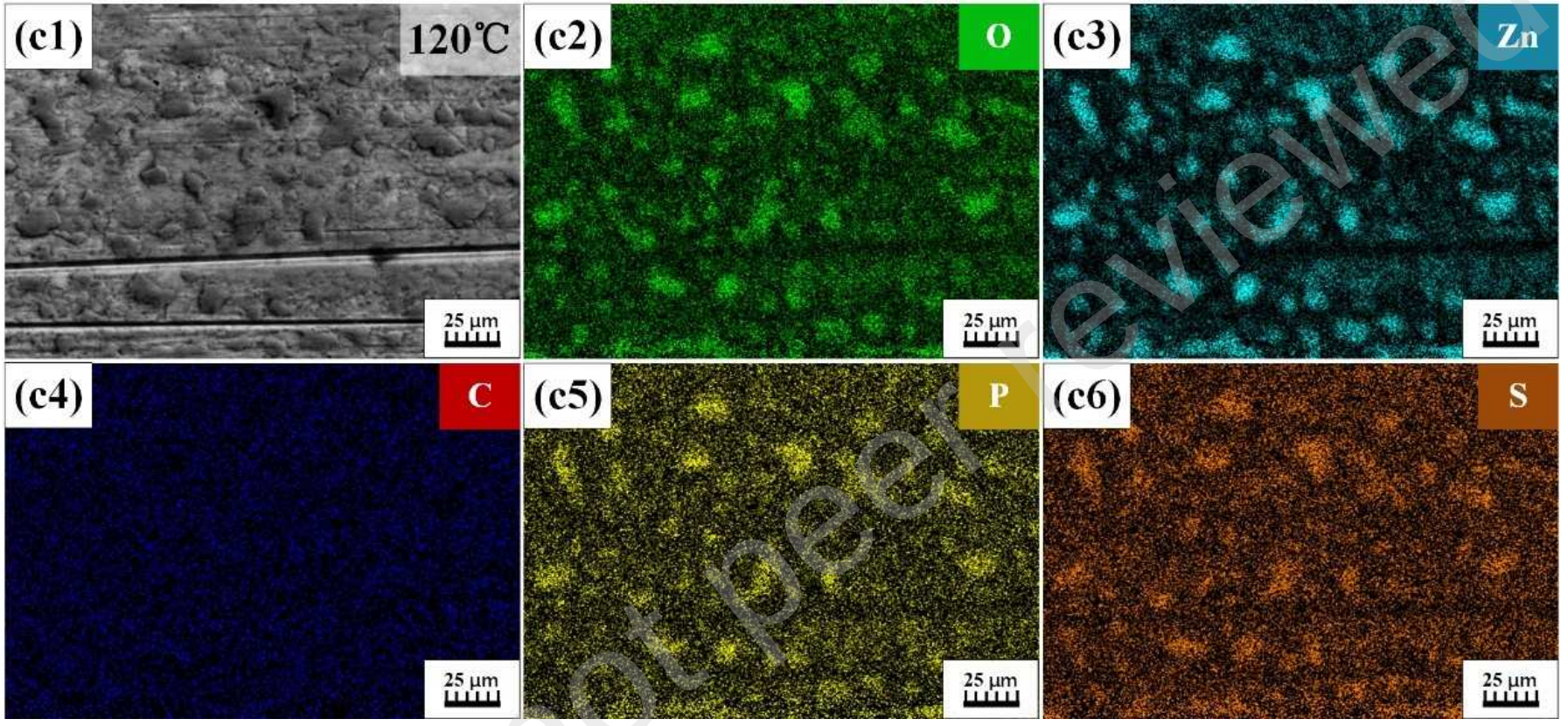

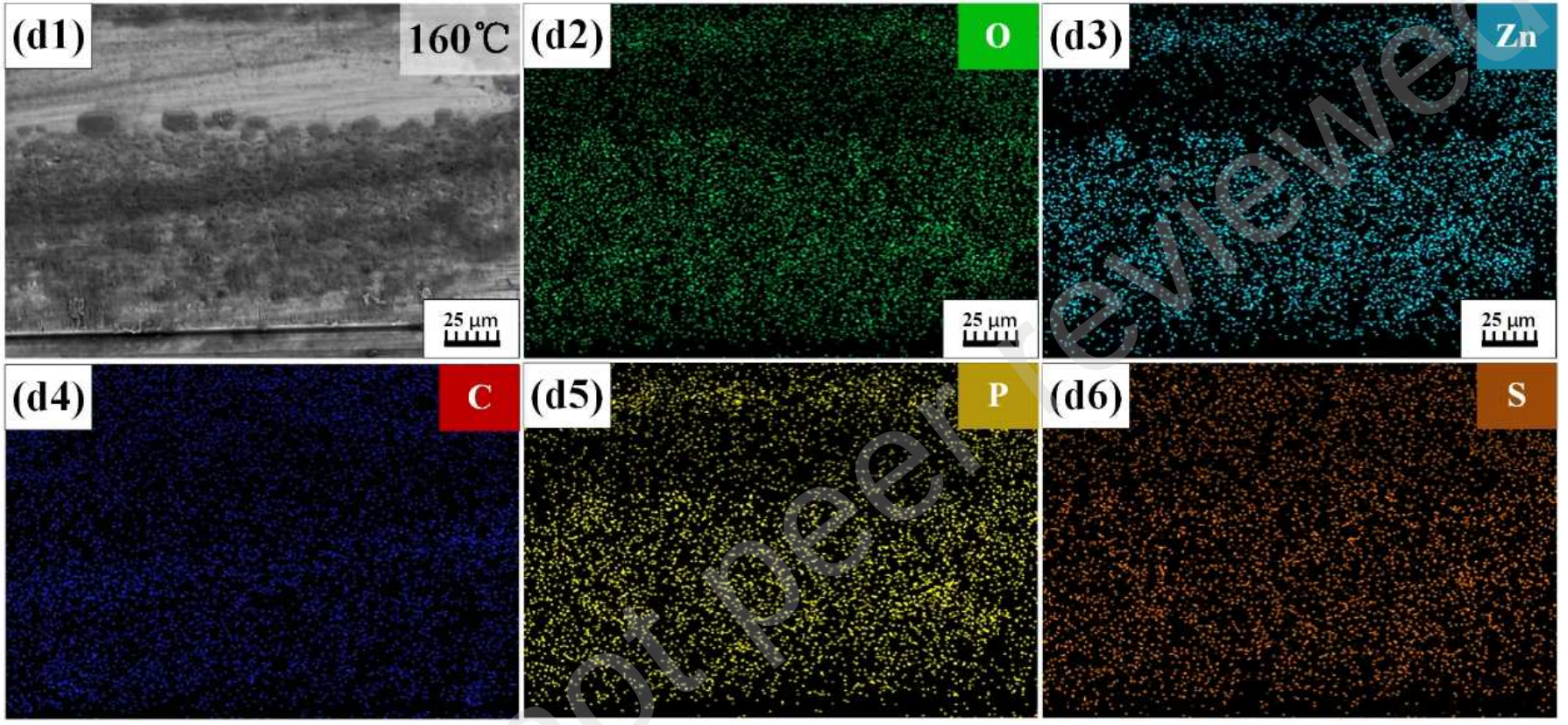

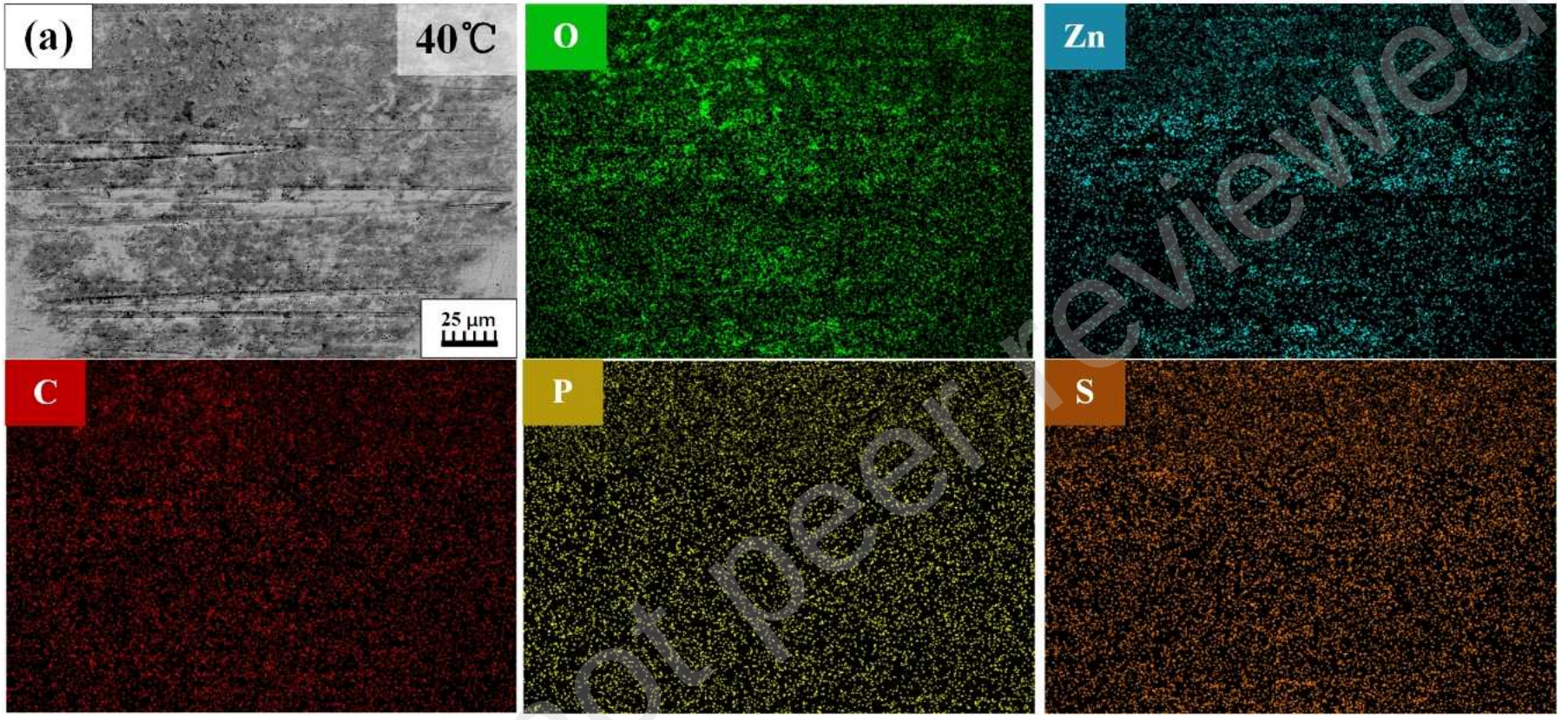

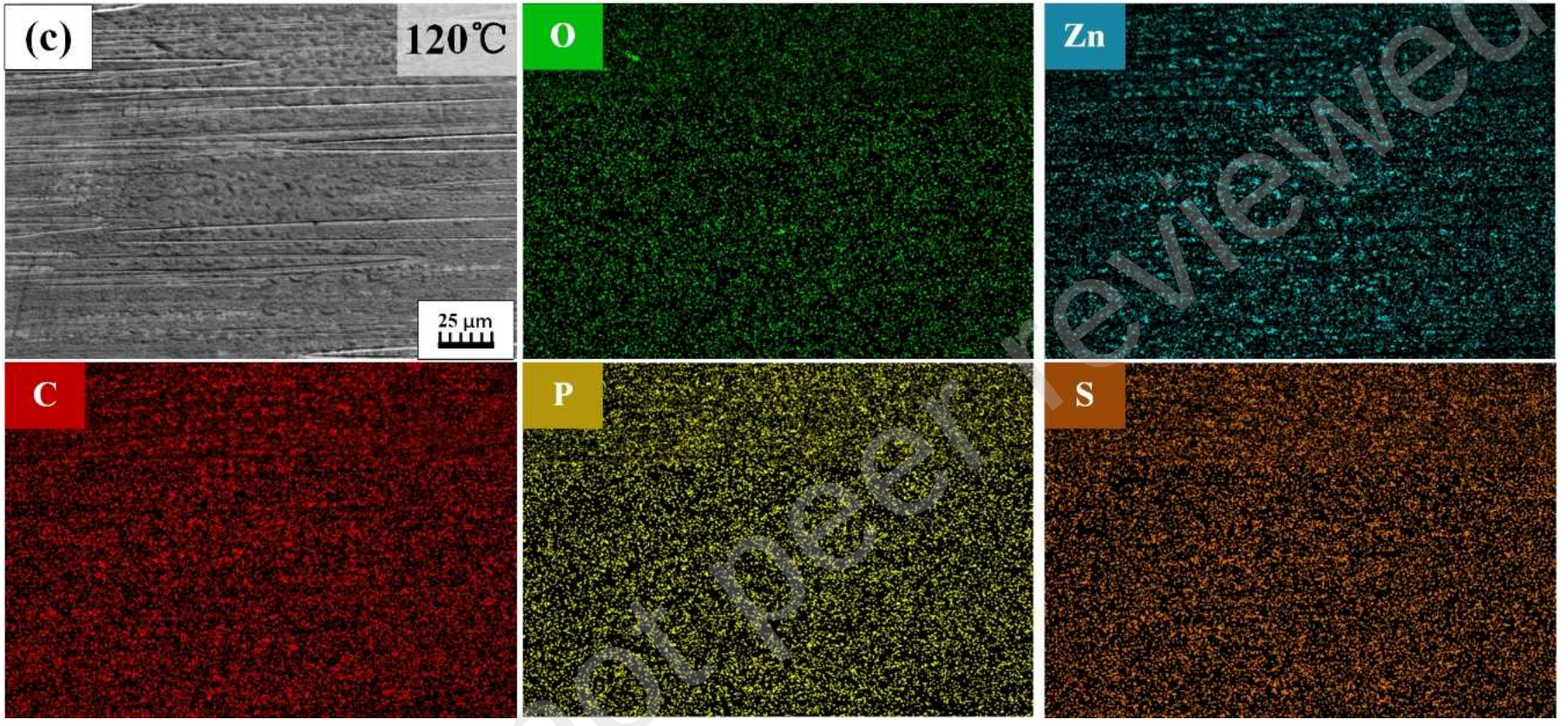

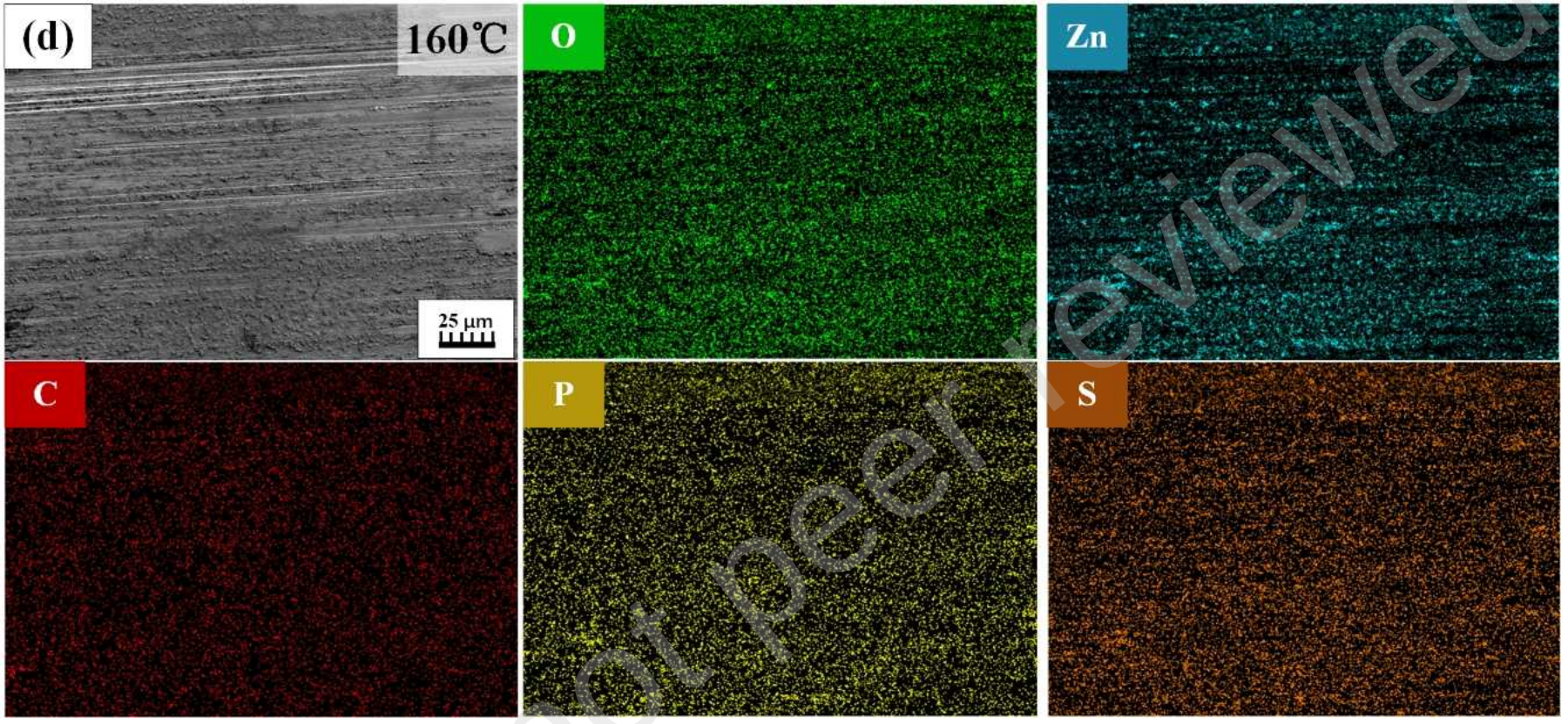

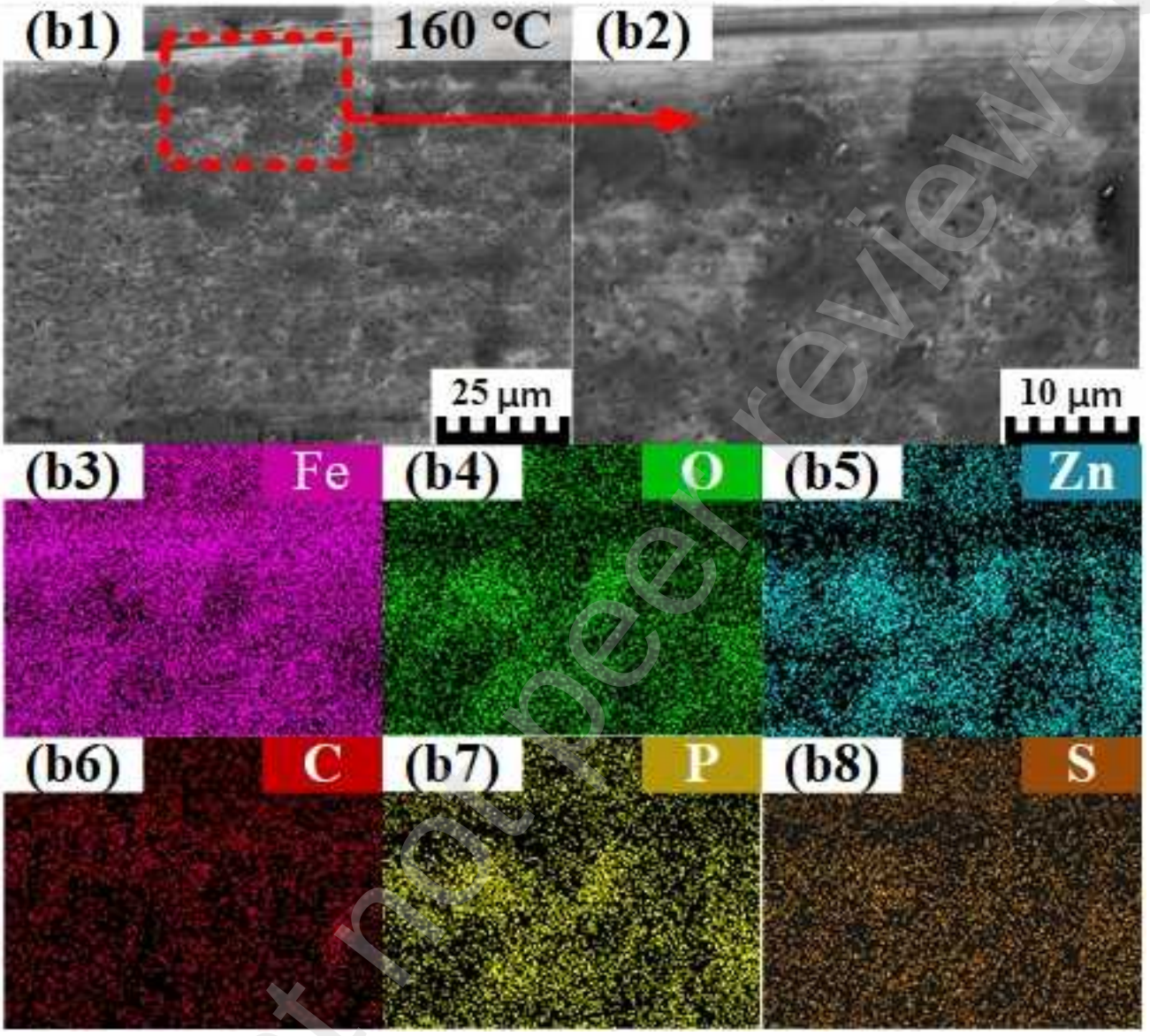

(b)